AD_____

Award Number: W81XWH-05-1-0051

TITLE: Anti-angiogenic action of neutral endopeptidase

PRINCIPAL INVESTIGATOR: David M. Nanus, M.D.

CONTRACTING ORGANIZATION: Weill Medical College of Cornell University
New York, NY 10065

REPORT DATE: November 2007

TYPE OF REPORT: Final

PREPARED FOR: U.S. Army Medical Research and Materiel Command
Fort Detrick, Maryland 21702-5012

DISTRIBUTION STATEMENT: Approved for Public Release;
Distribution Unlimited

REPORT DOCUMENTATION PAGE

Form Approved
OMB No. 0704-0188

1. REPORT DATE	2. REPORT TYPE	3. DATES COVERED
30-11-2007	Final	1 NOV 2004 - 31 OCT 2007

4. TITLE AND SUBTITLE
Anti-angiogenic action of neutral endopeptidase

5a. CONTRACT NUMBER

5b. GRANT NUMBER
W81XWH-05-1-0051

5c. PROGRAM ELEMENT NUMBER

6. AUTHOR(S)
David M. Nanus, M.D.

Email:

5d. PROJECT NUMBER

5e. TASK NUMBER

5f. WORK UNIT NUMBER

7. PERFORMING ORGANIZATION NAME(S) AND ADDRESS(ES)

Weill Medical College of Cornell University
New York, NY 10065

8. PERFORMING ORGANIZATION REPORT NUMBER

9. SPONSORING / MONITORING AGENCY NAME(S) AND ADDRESS(ES)
U.S. Army Medical Research and Materiel Command
Fort Detrick, Maryland 21702-5012

10. SPONSOR/MONITOR'S ACRONYM(S)

11. SPONSOR/MONITOR'S REPORT NUMBER(S)

12. DISTRIBUTION / AVAILABILITY STATEMENT
Approved for Public Release; Distribution Unlimited

13. SUPPLEMENTARY NOTES

14. ABSTRACT

See next page.

15. SUBJECT TERMS
Angiogenesis, Prostate Cancer, Basic fibroblast growth factor
Proteolysis, Vascular endothelial cells, Cell surface peptidase, Neutral endopeptidase

16. SECURITY CLASSIFICATION OF:			17. LIMITATION OF ABSTRACT	18. NUMBER OF PAGES	19a. NAME OF RESPONSIBLE PERSON
a. REPORT	b. ABSTRACT	c. THIS PAGE			USAMRMC
U	U	U	UU	30	19b. TELEPHONE NUMBER *(include area code)*

Abstract
Angiogenesis, or the formation of new blood vessels from existing vasculature is an important event in tumor progression. It results from a complex, multistep biochemical cascade that is initiated by the activation of endothelial cells in response to angiogenic factors. In prostate cancers, angiogenic factors are produced by epithelial and stromal cells, and are believed critical to prostate cancer growth and progression. One of the most important of these factors is basic fibroblast growth factor (bFGF), which plays an important role in angiogenesis through the stimulation of endothelial cell proliferation, migration, and protease production *in vitro* phenomenon. A number of studies both *in vitro* and in patient specimens suggest that enhanced expression of bFGF contributes to more aggressive prostate cancer. Clearly, a better understanding of the pathways regulating angiogenesis in the prostate and how these pathways change during malignant transformation and prostate cancer progression will assist in developing more effective therapies for patients with prostate cancer.
Cell-surface peptidases are the guardians of the cell against small stimulatory peptides, functioning to control growth and differentiation in normal cells by regulating peptide access to their cell-surface receptors. They are integral membrane proteins with their enzymatic site exposed to the external cell surface, Neutral endopeptidase (NEP) is a cell-surface peptidase normally expressed by prostatic epithelial cells, whose expression is lost in over half of prostate cancers. NEP substrates include small peptides that have been implicated in prostate cancer progression, including endothelin-1, bombesin and neurotensin. We have now reported that bFGF is also a substrate for NEP.
The goals of this application focus on deciphering the interaction between NEP and bFGF. We have now identified precisely how and where NEP cleaves bFGF, and the biological effects of these cleavage products on prostate cancer cells and human vascular endothelial cells. We are in the process of developing angiogenesis-based models in mice that have been engineered to lack the NEP gene allowing us to directly determine the contribution of NEP to angiogenesis. Studies are ongoing to assess the role of hypoxia on NEP action, and establish the relationship between NEP and other angiogenic factors such as heparin sulfate proteoglycans, vascular endothelial growth factor, and endothelin-1; and in epithelial and endothelial cells.
The results generated by our research are likely to contribute to a greater understanding of prostate cancer angiogenesis, and to explain, at least in part, the impact of NEP loss on bFGF expression. Moreover, this understanding potentially will have widespread applicability to not only other cancers, but to other angiogenic processes such as wound healing and ischemic vascular disease, where augmentation of angiogenesis (through inhibition of NEP) would be of therapeutic benefit. This improved understanding of NEP, bFGF and angiogenesis in prostate cancer may then be used in the design of novel therapeutic approaches.

Table of Contents

INTRODUCTION:

Neutral endopeptidase (NEP, CD10) is a cell-surface peptidase that is normally expressed by prostatic epithelial cells, and is lost in ~50% of prostate cancers.{10080} NEP possesses numerous anti-tumor actions, including catalytic inactivation of neuropeptides such as endothelin-1 and bombesin, and direct protein-protein interaction interactions with other proteins including the PTEN tumor suppressor protein and ezrin/radixin/moesin (ERM) proteins.{10131} Preliminary data suggested that NEP also possesses anti-angiogenic activity, and that this effect resulted from the fact that basic fibroblast growth factor (bFGF; FGF-2) is a previously unrecognized substrate for NEP. The aims of this project were to characterize the interaction between NEP and bFGF, and to delineate the anti-angiogenic action of NEP on human vascular endothelial cells. Understanding the regulation of angiogenesis is critical to developing strategies to inhibit tumor-related angiogenesis in prostate cancer.

BODY:

Task 1. To characterize the interaction between neutral endopeptidase (NEP) and basic fibroblast growth factor (bFGF)

a. *Develop a series of plasmids expressing wild type and mutant bFGF.*
b. *Perform assays to identify the specific sequence where NEP cleaves bFGF.*
c. *Assess the role of heparanoids in regulating bFGF susceptibility to proteolytic cleavage.*
d. *Characterize the actions of bFGF cleavage products on FGF receptor signal transduction pathways, and on the biology of human vascular endothelial cells.*
e. *Assess the pro-angiogenic activity of bFGF in NEP null mice compared to wild-type mice.*

A & B. *Develop a series of plasmids expressing wild type and mutant bFGF; and Perform assays to identify the specific sequence where NEP cleaves bFGF.*

To identify the site where NEP cleaves bFGF, we incubated bFGF and recombinant NEP (rNEP) with and without the NEP inhibitor CGS24592, and analyzed the reactions using matrix-assisted laser desorption ionization-time of flight (MALDI-TOF) mass spectrometry. This identified a specific 2019 Da band that corresponded to a 20 amino acid peptide located at the C-terminus of the bFGF protein. As a control, we performed the same digestion using either immunoprecipitated wildtype NEP (WT5) or enzymatically inactive NEP (M22) expressed using tetracycline-repressible promoter.{9460}, demonstrating that an intact enzyme activity is required to observe bFGF cleavage. Analysis of the bFGF amino acid sequence confirmed a potential NEP cleavage site between leucine 135 and glycine 136. Moreover, analysis of the amino acid sequence and the 3-dimensional structure of bFGF indicated that the NEP recognition site between leucine 135 and glycine 136 was located at the outer edge of the bFGF protein suggesting that it could fit into the NEP cleavage pocket. We then used cloning techniques to create a series of GST fusion proteins containing the full-length bFGF protein, each of its two cleavage products, and a mutated full-length bFGF protein that is resistant to NEP cleavage. (See *J Biol Chem:*281:33597-33605 in Appendix for detailed results and figures).

C. *Assess the role of heparanoids in regulating bFGF susceptibility to proteolytic cleavage.*

Basic FGF is primarily stored in the extracellular matrix and basement membrane associated with heparan sulfate proteoglycan (HSPG). Activity of bFGF is controlled in part by a low-affinity but high-capacity interaction with HSPG. Free bFGF may be proteolytically degraded, as suggested by in vitro reactivity of the C-terminal portion of bFGF to trypsin and chymotrypsin. We hypothesized that HSPG binding could function to protect bFGF from degradation by NEP since leucine 135 and glycine 136 of the bFGF protein lie within a basic region where heparin-derived tetra- and hexasaccharides have been reported to complex with bFGF. Since heparinoids interacts with bFGF resulting in its resistance to nonspecific proteolysis *in vitro,* we assessed the role of heparinoids in protecting bFGF from cleavage by NEP. We showed that heparin completely inhibited the ability of NEP to cleave bFGF. (See *J Biol Chem:*281:33597-33605 in Appendix for detailed results and figures).

D. *Characterize the actions of bFGF cleavage products on FGF receptor signal transduction pathways, and on the biology of human vascular endothelial cells.*

To establish that NEP antiangiogenic activity is a direct consequence of bFGF cleavage, we examined whether cleavage of bFGF abrogated its ability to signal through the fibroblast growth factor receptor (FGF-R). Upon engaging bFGF, FGF-R undergoes dimerization, autophosphorylation and then signals by way of the mitogen-activated protein kinase pathway resulting in extracellular signal-related kinase (ERK) phosphorylation. Utilizing the GST-bFGF fusion proteins, we determined the actions of bFGF cleavage products on FGF signaling through FGF receptor 2 (FGFR2), its predominant cognate receptor, and the effects of cleavage on human vascular endothelial cells growth and differentiation. We showed that neither the 1-135 nor the 136-155 bFGF cleavage products a) demonstrated any biologic activity in a capillary tube formation assay, and b) could induce bFGF signaling through the FGFR2 as determined by assaying ERK phosphorylation. Furthermore, mutation of the NEP cleavage site led to inhibition of bFGF stimulated capillary tube formation. (See *J Biol Chem:*281:33597-33605 in Appendix for detailed results and figures).

E. *Assess the pro-angiogenic activity of bFGF in NEP null mice compared to wild-type mice.*

We planned to assess the contribution of NEP to abrogating the pro-angiogenic activity of bFGF in neoplasia in NEP null mice compared to wild-type mice, using both a corneal pocket i*n vivo* angiogenesis assay as well as a chemical skin carcinogenesis model. We were unable to perform the corneal pocket assay in NEP null mice for technical reasons. However, we did perform chemical carcinogenesis assays. We tested in a cohort of wild type and null mice the effects of DMBA-induced skin carcinogenesis but failed to demonstrate an increased rate of conversion. Given that there was a 8% incidence of tumor formation the wild type and 14% incidence in the NEP null mice, considerably lower than that observed in other backgrounds (50-80%), we conclude that the assay will not be adequately powered statistically to detect a difference in our strain. We therefore took an alternative approach to examine angiogenesis and isolated endothelial cells from murine lung, hear and aorta using immunoselection with magnetic beads in order to compare NEP null and wild type endothelial cells. Neprilysin deficient vascular endothelial cells do not exhibit a resting endothelial cell morphology at confluence (Figure 1A) and exhibit anchorage-independent growth in soft agar under standard endothelial culture conditions (Figure 1B). Neutral endopeptidase expression is upregulated by the addition of serum (1C), consistent with androgen-induced expression seen in epithelial cells. In addition, neprilysin-deficient cells exhibit hyperphosphorylation of ERK under basal culture conditions, suggesting that the absence of neprilysin leads to the constitutive activation of upstream signaling molecules such as FGFR (1D). These data together with the observation that FGF-2 is an NEP substrate indicate a central role for NEP in the biology and function of vascular endothelium, and that targeting the NEP/FGF-2 axis in this cell type may represent a novel antiangiogenic therapeutic strategy.

Task 2. To delineate the anti-angiogenic action of NEP on human vascular endothelial cells.

a. Characterize the inhibitory effects of exogenous and endogenous NEP on angiogenesis.

b. *Decipher the hypoxic-dependent regulation of NEP expression in human vascular endothelial cells.*

A. *Characterize the inhibitory effects of exogenous and endogenous NEP on angiogenesis.*

Endogenous NEP expressed on human vascular endothelial cells negatively regulates bFGF-induced angiogenesis. Previous studies indicated that NEP is expressed by human vascular endothelial cells Analyses of HUVEC and SV-40 transduced human bone marrow endothelial cells (tHBMEC) revealed NEP enzyme specific activities of 36 pmol/mg/min and 197 pmol/mg/min, respectively. To assess the functional effect of endogenous NEP on bFGF-induced angiogenesis *in vitro*, we used tbe capillary tube formation assay to measure the effects of bFGF with and without the NEP inhibitor CGS24592 in

tHBMEC cells plated on matrigel coated plates. Cells grown in the presence of bFGF and CGS24592 demonstrated significantly more capillary tube formation compared to cells grown in bFGF alone, CGS24592 alone or the untreated negative control ($P<0.05$). We next assessed endothelial cell growth in tHBMEC treated with 600 pg/mL bFGF as a function of increasing concentrations of CGS24592. Transduced HBMEC incorporated more MTT in the presence of CGS24592, suggesting that inhibition of endogenous NEP activity results in increased bFGF-induced cell growth ($P<0.03$). Similar results were obtained for HUVEC cells.

Mutagenesis of the putative NEP cleavage site residues to alanine resulted in stepwise decrease in NEP cleavage, with the double mutant L135A/G136A demonstrating a near complete loss of cleavage by NEP. When tested in the matrigel tube formation, the NEP-resistant bFGF was capable of inducing tube formation on matrigel comparable to that seen with a 10-fold higher concentration of bFGF or with CGS24592 treatment. Taken together, these data suggest that endogenously expressed NEP on vascular endothelial cells regulates bFGF-induced angiogenesis. (See *J Biol Chem:*281:33597-33605 in Appendix for detailed results and figures).

We also assessed the effects of endogenously expressed NEP on angiogenesis by stably expressing lentiviral vectors encoding wild type NEP (L-NEP), catalytically inactive mutant NEP (L-NEPmu), and green fluorescent protein (L-GFP) in DU145 prostate cancer cells. Resulting expression of endogenous NEP, with a specific activity of 96.5 ± 10.2 pmol/μg/min, did not affect cell proliferation or invasiveness, while levels in cell culture supernatant of FGF-2 were decreased by 80% in DU145 cells infected with L-NEP compared to cells infected with L-NEPmu or L-GFP ($p < 0.05$). In vitro tubulogenesis of human vascular endothelial cells induced by conditioned media from DU145 cells infected with L-NEP was significantly reduced compared with that from DU145 cells infected with L-GFP ($p < 0.01$). Finally, tumor xenografts from L-NEP-infected DU145 cells were significantly smaller compared to control cell xenografts, as was vascularity within the tumors ($p < 0.05$). These data further demonstrated that stable expression of NEP inhibited prostate cancer tumorigenicity by inhibiting FGF-2 mediated angiogenesis. (See *Prostate Cancer Prostatic Dis.* 2007 epub. in Appendix for detailed results and figures).

B. *Decipher the hypoxic-dependent regulation of NEP expression in human vascular endothelial cells.*

Hypoxia is arguably the most important physiologic angiogenic stimulus. A previous report showed that NEP enzyme activity was significantly decreased after 24 - 48 hours of hypoxia in murine lung extracts. Moreover, hypoxia has been associated with a more aggressive phenotype and correlates with enhanced Akt phosphorylation in prostate cancer cells. To determine if NEP was regulated by hypoxia in prostate cancer cells and human vascular endothelial cells, we incubated these cells in media containing 125 μM $CoCl_2$ which simulates hypoxic conditions over time. As shown in Figure 2, NEP enzyme activity decreased significantly in LNCaP cells and in HUVEC cells, although the degree of decrease is less apparent in HUVEC cells as they produce less NEP enzyme activity. These data suggest that NEP activity decreases under hypoxic conditions, which should lead to increased bFGF-induced signaling and angiogenesis.

Examination of NEP protein expression by Western blotting in cells incubated in a sealed hypoxia chamber confirmed a decrease in NEP protein expression, which mirrored the decrease in NEP enzyme activity (Figure 3), indicating that hypoxic regulation of NEP is likely at the transcriptional or translational level. Using quantitative real time PCR, we next measured the relative message levels of NEP in hypoxia treated PC cells. Messenger RNA levels of NEP decreased between 50-75% relative to normoxic controls with high statistical significance (Figure 4), indicating that hypoxic regulation of NEP is likely transcriptional.

Transcriptional regulation of gene expression by hypoxia is typically mediated by the binding of hypoxia inducible factor complex to hypoxia inducible elements. This mechanism has been implicated in the regulation of many hypoxia-responsive genes, including VEGF, ET-1, and the androgen receptor. The HRE has the canonical structure 5'-BACGTSSK-3' where B=G/C/T, S=G/C. and K=G/T and is typically

located immediately upstream of the transcriptional initiation site. Hypoxic gene regulation may be modulated by other signal transduction pathways, including the MAP kinase cascade. Examination of the NEP gene revealed two potential HREs within 10 kilobases of the transcriptional start site, along with six potential intronic elements (Figure 5).

KEY RESEARCH ACCOMPLISHMENTS:

1) NEP functions as an antiangiogenic agent *in vivo* by direct proteolytic cleavage of bFGF resulting in its inactivation with concomitant loss of ability to bind to cell surface receptors and induce phosphorylation of MAP kinase, its predominant downstream target.
2) Previous studies indicated that NEP substrates were $\leq$ 41 amino acid in length. NEP can cleave and inactivate a substrate > 150 amino acids suggesting there are other as yet unknown NEP substrates.
3) Binding of bFGF with heparan sulfate proteoglycan protects bFGF from NEP proteolytic cleavage.
4) Full length basic FGF protein with a mutated NEP recognition site is a potent inducer of angigenesis.
5) Endogenous NEP activity decreases under hypoxic conditions.

REPORTABLE OUTCOMES:

Goodman, Jr. O.B., Febbraio M., Simantov R., Zheng R., Shen R., Silverstein R.L., Nanus DM. (2006) Neprilysin inhibits angiogenesis via proteolysis of fibroblast growth factor-2. *J Biol Chem* 281, 33597-605.

Horiguchi A, Chen DYT, Goodman OB, Zheng R, Shen R, Guan H, Hersh LB, Nanus DM. Neutral endopeptidase inhibits prostate cancer tumorigenesis by reducing FGF-2-mediated angiogenesis. *Prostate Cancer Prostatic Dis*. 2007, in press.

FUNDING:

1) DOD W81XWH07 $702,000 8/1/07 (OG/DN)
2) American Society of Clinical Oncology Young Investigator Award (7/2005- 6/2006) $35,000 (OG/DN)

CONCLUSION:

Prostate cancer is the most common primary cancer among men and the second leading cause of cancer deaths in males in the United States. Our studies show that NEP loss is involved in the development and progression of both early and advanced hormone refractory PC. Moreover, we have shown that complete loss of NEP expression in primary PC is associated with a shorter time to PSA recurrence, suggesting that in addition to NEP loss contributing to neuropeptide-mediated PC progression, it permits more effective malignant angiogenesis. Understanding the molecular events involved in the development and progression of PC is critical to developing more effective therapies. The studies supported by this award has directly led to a better understanding of the involvement of NEP in the development and progression of PC. These data provide support for novel antioangiogenic approaches for the treatment of advanced PC using NEP. Moreover, they provide a rationale to study the relationship of NEP and bFGF in non-malignant conditions (such as wound healing, ischemic vascular disease) where angiogenesis is pathologically impaired in order to design more effective approaches to stimulate healing (such as a “super bFGFs” which resist proteolysis by NEP and therefore may be a more potent angiogenic agent).

APPENDICES:

1) Reprints of published manuscripts.
2) Figures

THE JOURNAL OF BIOLOGICAL CHEMISTRY VOL. 281, NO. 44, pp. 33597–33605, November 3, 2006

Neprilysin Inhibits Angiogenesis via Proteolysis of Fibroblast Growth Factor-2*

Received for publication, March 16, 2006, and in revised form, August 14, 2006 Published, JBC Papers in Press, August 28, 2006, DOI 10.1074/jbc.M602490200

Oscar B. Goodman, Jr.[‡§1], Maria Febbraio[¶], Ronit Simantov[‖], Rong Zheng[‡§], Ruoqian Shen[‡], Roy L. Silverstein[¶], and David M. Nanus[‡§2]

From the [‡]Urologic Oncology Research Laboratory, Department of Urology and the [§]Division of Hematology and Medical Oncology, Department of Medicine, Weill Medical College of Cornell University-New York Presbyterian Hospital, New York, New York 10021, [¶]Lerner Research Institute, Cleveland Clinic Foundation, Cleveland, Ohio 44195, and [‖]Bayer Pharmaceuticals, Inc., West Haven, Connecticut 06516-4175

Neprilysin is a cell surface peptidase that catalytically inactivates neuropeptide substrates and functions as a tumor suppressor via its enzymatic function and multiple protein-protein interactions. We investigated whether neutral endopeptidase could inhibit angiogenesis *in vivo* utilizing a murine corneal pocket angiogenesis model and found that it reduced fibroblast growth factor-2-induced angiogenesis by 85% ($p < 0.01$) but had no effect on that of vascular endothelial growth factor. Treatment with recombinant neprilysin, but not enzymatically inactive neprilysin, resulted in a slight increase in basic fibroblast growth factor electrophoretic mobility from proteolytic cleavage between amino acids Leu-135 and Gly-136, which was inhibited by the neutral endopeptidase inhibitor CGS24592 and heparin. Cleavage kinetics were rapid, comparable with that of other known neprilysin substrates. Functional studies involving neprilysin-expressing vascular endothelial cells demonstrated that neutral endopeptidase inhibition significantly enhanced fibroblast growth factor-mediated endothelial cell growth, capillary array formation, and signaling, whereas exogenous recombinant neprilysin inhibited signaling. Recombinant constructs confirmed that cleavage products neither promoted capillary array formation nor induced signaling. Moreover, mutation of the cleavage site resulted in concomitant loss of cleavage and increased the potency of fibroblast growth factor-2 to induce capillary array formation. These data indicate that neprilysin proteolytically inactivates fibroblast growth factor-2, resulting in negative regulation of angiogenesis.

Neprilysin (neutral endopeptidase 24.11, CD10) is a 90–110-kDa cell surface peptidase normally expressed by a variety of tissues, including epithelial cells of the prostate, kidney, intestine, endometrium, adrenal glands, and lung. This enzyme cleaves peptide bonds on the amino side of hydrophobic amino acids and inactivates a variety of physiologically active peptides, including atrial natriuretic factor, substance P, bradykinin, oxytocin, Leu- and Met-enkephalins, neurotensin, bombesin, endothelin-1, and β-amyloid. Loss or a decrease in neprilysin expression has been reported in a variety of malignancies, including renal cancer, invasive bladder cancer, poorly differentiated stomach cancer, small cell and non-small cell lung cancers, endometrial cancer, and prostate cancer (1, 2). Reduced expression of cell surface peptidases such as neprilysin results in the accumulation of higher peptide concentrations that mediate neoplastic progression (3).

Using prostate cancer as a model to study the involvement of neprilysin in malignancy, we have demonstrated the following. 1) Neprilysin protein expression is absent in nearly 50% of primary prostate cancers (2). 2) Neprilysin inhibits neuropeptide-mediated cell growth, cell migration, and ligand-independent activation of the insulin-like growth factor-1 receptor leading to Akt phosphorylation (1, 4). 3) Neprilysin can inhibit cell migration independently of its catalytic activity via protein-protein interaction of its cytoplasmic domain with tyrosine-phosphorylated Lyn kinase, which then binds the p85 subunit of phosphatidylinositol 3-kinase resulting in an neprilysin-Lyn-phosphatidylinositol 3-kinase protein complex. This complex competitively blocks the interaction between focal adhesion kinase and phosphatidylinositol 3-kinase (5). 4) Neprilysin directly binds to ezrin/radixin/moesin proteins resulting in decreased binding of ezrin/radixin/moesin proteins to the hyaluronan receptor CD44, such that cells expressing neprilysin demonstrate decreased cell adhesion and cell migration (6). 5) Neprilysin directly interacts with the PTEN tumor suppressor protein, recruiting endogenous PTEN to the cell membrane, leading to prolonged PTEN protein stability and increased PTEN phosphatase activity and resulting in a constitutive down-regulation of Akt activity (7). 6) Neprilysin expression inhibits tumorigenicity in an animal model of prostate cancer (8). Taken together, these studies have demonstrated that neprilysin protein functions to suppress and inhibit many processes that contribute to neoplastic progression.

Enzymatically active neprilysin is also expressed by vascular endothelial cells of venous and arterial origin (9). The neprilysin substrate endothelin-1 has previously been shown to act directly on endothelial cells via the ET_B receptor to modulate different stages of neovascularization, including proliferation, migration, invasion, protease production, and morphogenesis,

* This work was supported in part by National Institutes of Health Grant CA80240, DOD Grant PC040758, and the Robert H. McCooey Memorial Cancer Research Fund. The costs of publication of this article were defrayed in part by the payment of page charges. This article must therefore be hereby marked "*advertisement*" in accordance with 18 U.S.C. Section 1734 solely to indicate this fact.

[1] Supported by a fellowship from the Sass Foundation for Medical Research and an American Society of Clinical Oncology Young Investigator Award.

[2] To whom correspondence should be addressed: Weill Medical College of Cornell University, 525 E. 68th St., ST-359, New York, NY 10021. Tel.: 212-746-3152; Fax: 212-746-6645; E-mail: dnanus@med.cornell.edu.

resulting in neovascularization *in vivo* (10). Based on these observations, we investigated whether neprilysin also functions as an antagonist of angiogenesis. We report here that neprilysin is indeed anti-angiogenic *in vivo*, significantly inhibiting angiogenesis. Surprisingly, we demonstrate that neprilysin catalytically inactivates the potent angiogenic factor, fibroblast growth factor-2 (FGF-2).[3] This is the first report of an enzyme that specifically cleaves and inactivates FGF-2, resulting in inhibition of angiogenesis *in vivo*, further demonstrating the potent tumor-suppressive function of neprilysin.

EXPERIMENTAL PROCEDURES

Cell Lines and Reagents—LNCaP cells were maintained in RPMI 1640 medium with 10% fetal calf serum (FCS) supplemented with penicillin (100 IU/ml) and streptomycin (100 μg/ml). Human umbilical vein endothelial cells (HUVEC) were isolated as previously described (11) and maintained in M199 medium (Invitrogen) supplemented with 10 units/ml heparin sodium, 10% FCS (Gemini), 2 mM L-glutamine, 100 μg/μl ECGS (Biomedical Technology) supplemented with penicillin and streptomycin. SV40-transduced human bone marrow microvascular endothelial cells (tHBMEC, kindly provided by Dr. Babette Weksler, Weill Medical College) were maintained in Dulbecco's modified Eagle's medium supplemented with 5% FCS as previously described (12). Vascular endothelial growth factor (VEGF) and growth factor-reduced Matrigel were purchased from BD Biosciences, and recombinant fibroblast growth factor-2 was purchased from Research Diagnostics, Inc.

Proteolysis and Mass Spectrometry—Commercially available recombinant FGF-2 was incubated at a concentration of 5–13 μM with recombinant neprilysin (rNEP; Arris Pharmaceutical, Inc.) at a concentration of 0.4–1.0 μM in 100 mM Tris-HCl, pH 7.6, buffer for 1 h at 25 °C in the presence or absence of 10 μM the specific neprilysin inhibitor CGS24592 (Novartis Pharmaceutical, Inc.) or 12 units/ml heparin sulfate. Reaction aliquots were analyzed by 14% SDS-PAGE with Coomassie Blue staining or by matrix-assisted laser desorption ionization time-of-flight mass spectrometry (MALDI-TOF MS; Micromass) in the mass spectroscopy core facility of Weill Medical College.

GST-FGF-2 and Maltose-binding Protein-FGF-2 Fusion Proteins—Full-length human FGF-2 cDNA (kindly provided by Dr. Daniel Rifkin, New York University Medical Center) was used as template to amplify the entire FGF-2 cDNA, which was then subcloned into pGEX-2T (Amersham Biosciences) and pMAL-2Cx (New England Biolabs) vectors using PCR primers containing restriction sites to enable directional cloning. The following amplimers were used: 5′-ACCATGGCAGCCGGGAGCATC-3′ (sense) and 5′-ATATGAATTCTCAGCTCTTAGCAGACATGGAAGAAAG-3′ (antisense) for glutathione *S*-transferase (GST) fusion proteins and 5′-ATGGCAGCCGGGAGCATC-3′ (sense) and 5′-CCCCAAGCTTTTAGCTCTTAGCAGACAT-3′ (antisense) for maltose-binding protein fusion proteins, as previously described (13). For GST constructs, the PCR product was then purified and digested with EcoRI and BamHI, generating the BamHI-EcoRI fragment corresponding to amino acids 136–155 and a BamHI-BamHI fragment corresponding to amino acids 1–135 of the FGF-2 protein. The restriction fragments were subcloned into pGEX-2T to generate GST fusion proteins with FGF-2 amino acids 1–155 (full-length), 1–135 (N-terminal neprilysin cleavage product), and 136–155 (C-terminal neprilysin cleavage product), and DNA sequencing was performed to confirm their accuracy. For maltose-binding protein constructs, the PCR product was digested with HindIII and XmnI and subcloned into the pMAL-2Cx vector. Fusion proteins of GST and maltose-binding protein with FGF-2 were expressed and purified from *Escherichia coli* BL21 cells using glutathione-agarose beads (Sigma) or amylase beads (New England Biolabs) as described (14). Protein content of the beads and 10 mM glutathione eluants were determined by densitometric analysis of Coomassie-stained SDS-PAGE gels against bovine serum albumin standards (NIH ImageJ software). In some experiments FGF-2 was cleaved from amylose beads (1 mg of total fusion protein) by digestion with 2 units of Factor Xa in Tris-buffered saline buffer and affinity purified using heparin-Sepharose chromatography (15). Site-directed mutants (L135A, G136A, and L135A/G136A) of the neprilysin cleavage site on FGF-2 were generated using a QuikChange mutagenesis kit (Stratagene) according to the manufacturer's instructions (mutagenic primers available upon request).

Matrigel Capillary Array Formation Assay—Transduced human bone marrow microvascular endothelial cells (12) or HUVEC were plated in 96-well plates at a density of 15,000 cells/well in Dulbecco's modified Eagle's medium containing 5% FCS, penicillin, streptomycin, and L-glutamine over 50 μl of polymerized growth factor-reduced Matrigel (10 mg/ml). CGS24592 at a concentration of 0.5–10 nM, phosphoramidon (30 μM; Sigma), or an equivalent volume of dimethyl sulfoxide vehicle (Me_2SO) was added to inhibit neprilysin activity for 2 h, followed by FGF-2 proteins at 0.3–50 nM concentrations. Cells were photographed after 4–18 h and measurements of capillary cord length obtained for multiple fields using ImageJ software and expressed as mean ± S.E. Statistical analyses of replicates were performed using unpaired two-tailed *t* testing (Prism Graph, GraphPad software).

MTT Growth Assay—Transduced human bone marrow microvascular endothelial cells plated in 96-well plates at a density of 1000 cells/well in Dulbecco's modified Eagle's medium containing 5% FCS, penicillin, streptomycin, L-glutamine, and 600 pg/ml FGF-2 were treated with increasing concentrations of CGS24592. Growth assays with 3-(4,5-dimethylthiazol-2-yl)-2,5-diphenyltetrazolium bromide (MTT) were performed after 48–96 h as described (16).

Corneal Pocket Assay—Hydron (Hydro Med Sciences, Cranbury, NJ) and sucralfate (Teva Pharmaceuticals, North Wales, PA) pellets of <1 μl were formulated with combinations of FGF-2 (10 ng or 50 ng/pellet), VEGF (200 ng/pellet), and rNEP

[3] The abbreviations used are: FGF-2, fibroblast growth factor-2; ERK, extracellular-regulated kinase; FCS, fetal calf serum; GST, glutathione *S*-transferase; HSPG, heparan sulfate proteoglycan; HUVEC, human umbilical vein endothelial cell; MALDI-TOF, matrix-assisted laser desorption ionization time-of-flight; MTT, methyl-thiazol-tetrazolium; rNEP, recombinant neprilysin; tHBMEC, SV40-transduced human bone marrow microvascular endothelial cells; VEGF, vascular endothelial growth factor; CHAPS, 3-[(3-cholamidopropyl)dimethylammonio]-1-propanesulfonic acid.

(50 or 100 ng/pellet) and implanted into corneas of C57BL/6 mice 0.5–1.0 mm from the limbus as described (17). Angiogenesis was assessed by slit-lamp microscopy 5 days after implantation (18). Statistical analysis of replicates was performed using a two-tailed unpaired *t* test (Prism Graph, GraphPad software). Studies were approved by the Institutional Animal Care Use Committee of Weill Medical College of Cornell University.

Neprilysin Enzyme Assays—Neprilysin enzyme activity determinations were performed as previously described (1) Briefly, subconfluent cells were rinsed in cold lysis buffer (50 mm Tris, pH 7.0, 150 mm NaCl) and lysed in lysis buffer containing 0.5% CHAPS (3-[3-cholamidopropyl-dimethylammonio]-1-propane-sulfonate). Protein concentrations were measured using the Bio-Rad DC protein assay kit (Bio-Rad Laboratories). Total neprilysin activity was assayed colorimetrically, and specific activities representing an average of six independent measurements were expressed in units of pmol/μg protein/min.

Western Blotting for GST, Total, and Phosphorylated Extracellular-regulated Kinase (ERK)—Subconfluent monolayers of tHBMEC, HUVEC, and LNCaP cells were lysed in radioimmune precipitation lysis buffer (50 mM Tris-HCl, pH 7.4, 1%v/v Nonidet P-40, 0.25% w/v sodium deoxycholate, 150 mM sodium chloride, 1 mM EDTA, 1 mM phenylmethylsulfonyl fluoride, 1 μg/ml each of aprotinin, leupeptin, pepstatin, 2 mM sodium orthovanadate) following 2-h pretreatment with 10 nM CGS24592 or vehicle and then treated for 20 min with various combinations of FGF-2, GST, or GST-FGF-2 fusion proteins, and rNEP as indicated. Lysates (50 μg each) were subjected to 10% SDS-PAGE, transferred to nitrocellulose membranes, blocked for 0.5 h, and blotted in 3% bovine serum albumin Tris-buffered saline with 0.1% Tween 20 using either anti-GST antibody (B14; 1:1000; Santa Cruz Biotechnology) or anti-phospho-ERK (197G2; 1:500; Cell Signaling Technology) as indicated for 1 h. This was followed by appropriate horseradish peroxidase-conjugated secondary antibody (sheep anti-mouse for B14 or donkey anti-rabbit for 197G2; Amersham Biosciences) at 1:4000 dilution for 0.5 h, enhanced chemoluminescence (Amersham Biosciences), and exposure to Kodak Biomax XAR film. Anti-phospho-ERK blots were stripped in 62.5 mM Tris-Cl, pH 6.8, 100 mM β-mercaptoethanol, 2% SDS, and reprobed with anti-ERK (C14; 1:1000; Santa Cruz) followed by anti-rabbit horseradish peroxidase secondary antibody. Films were scanned using an HP scanner and subjected to densitometric analysis using ImageJ and GraphPad software.

RESULTS

Neprilysin Cleaves FGF-2 Protein between Residues Leucine 135 and Glycine 136—To test the hypothesis that neprilysin could regulate angiogenesis *in vivo*, we used the murine corneal pocket assay to study the effect of rNEP on neovascularization induced by either FGF-2 or VEGF. In this assay, hydron pellets containing various concentrations of FGF-2 were implanted in the cornea ~1 mm from the limbus and neovascularization measured 5 days later. As shown in Fig. 1, rNEP significantly inhibited FGF-2-induced neovascularization ($p < 0.01$) but had no effect on that of VEGF. These results suggested the possibility that FGF-2 was inactivated catalytically by neprilysin. Basic

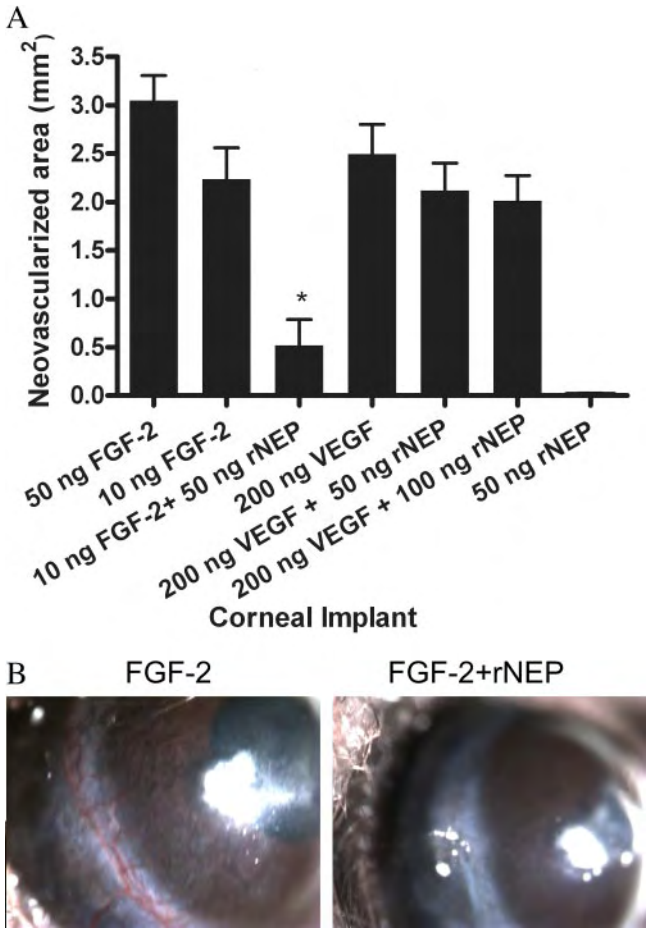

FIGURE 1. **Recombinant neprilysin inhibits FGF-2-induced, but not VEGF-induced, angiogenesis.** *A*, hydron pellets containing 50 ng of FGF-2 (positive control), 10 ng of FGF-2, 10 ng of FGF-2 + 50 ng of rNEP, 200 ng of VEGF, 200 + 50 ng of rNEP, 200 + 100 ng of rNEP, or 50 ng of rNEP alone (negative control) were implanted in the cornea of C57/B6 mice and new vessel formation at 5 days measured by slit lamp ophthalmoscopy. Statistical analysis of six eyes (three mice) in two independent experiments (a total of six mice for each group) was performed (* denotes $p <$ 0.01 compared with 10 ng of FGF-2, two-tailed unpaired *t* test). *B*, photograph of representative corneas: 10 ng of FGF-2 alone on *left*, 10 ng of FGF-2 + 50 ng of rNEP on *right*.

FGF is a potent proangiogenic, heparin-binding growth factor, with a primary translation product of 155 amino acids. Neprilysin hydrolyzes peptide bonds on the amino side of neutral residues; however, a protein of 155 amino acids is theoretically too large to be a substrate for neprilysin, as previous identified substrates are less than 43 amino acids (19, 20). To test whether neprilysin could hydrolyze FGF-2, we incubated rNEP with recombinant FGF-2 for 1 h and separated the products on a 14% polyacrylamide gel. Recombinant VEGF was used as control. As shown in Fig. 2*A*, *lane 1*, *arrow*), the molecular weight of FGF-2 protein, but not VEGF protein, was appreciably lower following rNEP incubation. The increased electrophoretic mobility of FGF-2 incubated with rNEP was blocked by the specific neprilysin inhibitor CGS24592 (21), indicating that neprilysin and not a contaminating protease cleaved FGF-2 (Fig. 2*B*, *lane 4*). To confirm neprilysin specifically cleaves FGF-2, we performed the same digestion using either immunoprecipitated wild-type neprilysin (WT5) or enzymatically inactive neprilysin

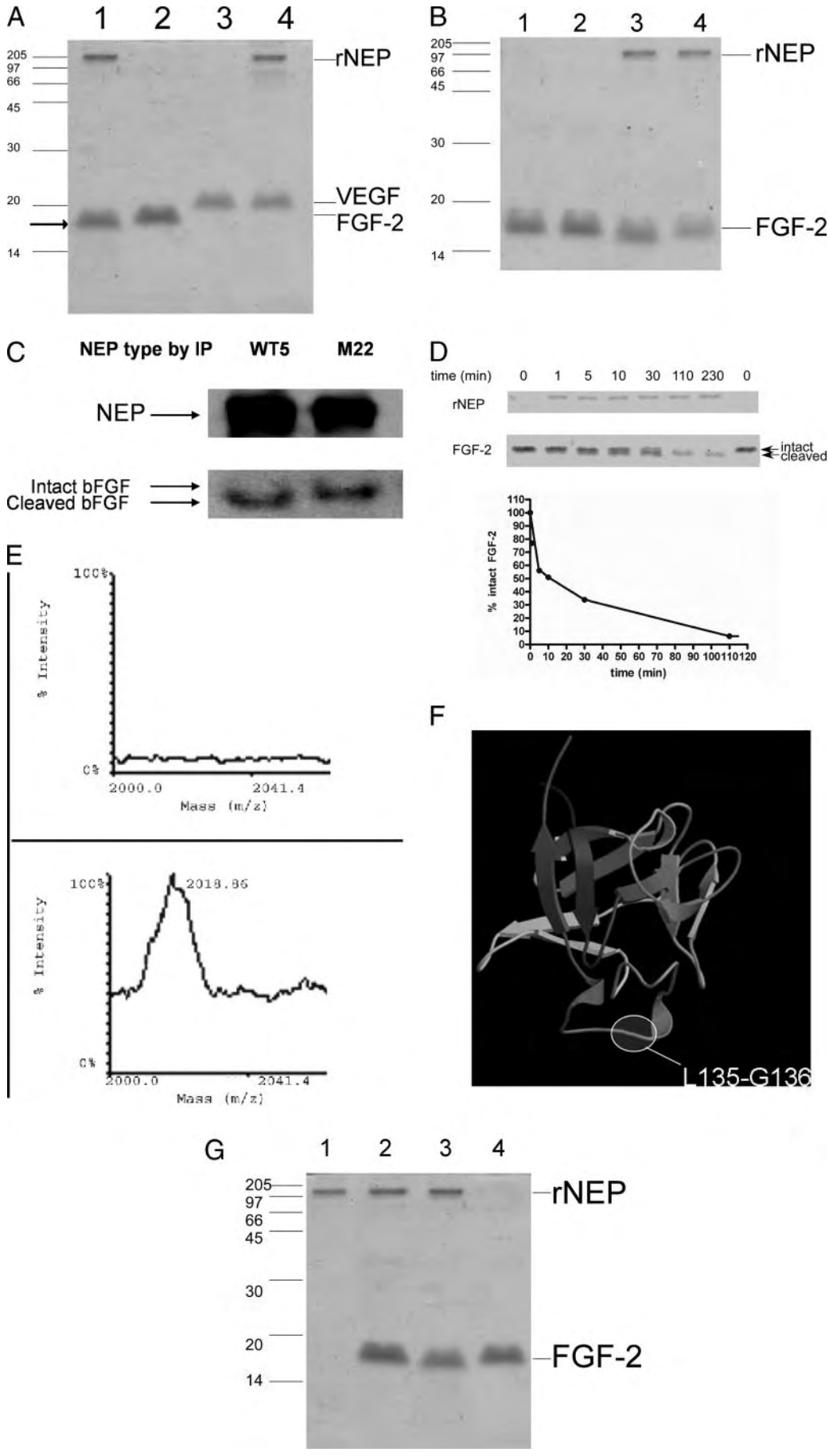

(M22) expressed using tetracycline-repressible promoter (4) and demonstrated that an intact enzyme activity is both necessary and sufficient to observe FGF-2 cleavage (Fig. 2*C*).

To confirm that FGF-2 cleavage occurs rapidly under physiologically relevant conditions, we assessed the kinetics of FGF-2 proteolysis by neprilysin, using an enzyme:substrate ratio of 1:30 and monitoring reaction progression using SDS-PAGE. As shown in Fig. 2*D*, 50% of FGF-2 was cleaved within the first 5–10 min, indicating rapid reaction kinetics.

Next the neprilysin cleavage site on FGF-2 was localized. Fibroblast growth factor-2 and rNEP were combined with or without the neprilysin inhibitor CGS24592 and analyzed using MALDI-TOF mass spectrometry. This identified a specific 2019-Da band produced in the absence of CGS24592 that corresponded precisely to a 20-amino acid peptide located at the C terminus of the FGF-2 protein (Fig. 2*E*). Examination of the FGF-2 amino acid sequence confirmed the potential neprilysin cleavage site between leucine 135 and glycine 136 (22). Correlation with the three-dimensional structure of FGF-2 (23) indicated that the neprilysin recognition site was located at the outer edge of the FGF-2 protein, suggesting that it could fit into the neprilysin active site (Fig. 2*F*).

Basic FGF is primarily stored in the extracellular matrix and basement membrane associated with heparan sulfate proteoglycan (HSPG). Activity of FGF-2 is controlled in part by a low affinity but high capacity interaction with HSPG. Free FGF-2 may be proteolytically degraded, as suggested by *in vitro* reactivity of the C-terminal portion of FGF-2 to trypsin and chymotrypsin (24, 25). We hypothesized that HSPG binding could protect FGF-2 from degradation by neprilysin because leucine 135 and glycine 136 of the FGF-2 protein lie within a basic region where heparin-derived tetra- and hexasaccharides have been reported to complex with FGF-2 (26). Incubation of rNEP and FGF-2 plus heparin (12 units/ml) showed that heparin completely inhibited the ability of neprilysin to cleave FGF-2 (Fig. 2*G*, *lane 2* compared with *lane 3*). Together, these data suggest that FGF-2 is a neprilysin substrate and that HSPG protects FGF-2 from neprilysin cleavage.

Endogenous Neprilysin Expressed on Human Vascular Endothelial Cells Negatively Regulates FGF-2-induced Angiogenesis—Previous studies indicate that neprilysin is expressed by human vascular endothelial cells (9, 27). Analyses of SV40 tHBMEC (12) and HUVEC revealed neprilysin enzyme-specific activities of 197 pmol/μg/min and 36 pmol/μg/min, respectively (data not shown). To assess the functional effect of endogenous neprilysin on FGF-2-induced angiogenesis *in vitro*, we used a capillary array formation assay to measure the effects of FGF-2 with and without the neprilysin inhibitor CGS24592 in tHBMEC cells plated on Matrigel-coated plates. As shown in Fig. 3*A*, cells grown in the presence of FGF-2 and CGS24592 demonstrated significantly more arrays compared with cells grown in FGF-2 alone, CGS24592 alone, or the untreated negative control ($p < 0.05$). We next assessed endothelial cell growth in tHBMEC treated with 600 pg/ml FGF-2 and with increasing concentrations of CGS24592. Transduced HBMEC incorporated more MTT as a function of CGS24592 concentration, suggesting that inhibition of endogenous neprilysin activity results in increased FGF-2-induced cell growth ($p < 0.03$, Fig. 3*B*). Similar results were obtained for HUVEC cells (data not shown). These data show that neprilysin expressed on vascular endothelial cells regulates FGF-2-induced angiogenesis.

FGF-2 Cleavage Products Do Not Induce Angiogenesis—To confirm that neprilysin cleavage blocks FGF-2 function, we produced and purified GST proteins fused to full-length FGF-2, FGF-2 cleavage products corresponding to amino acids 1–135 and 136–155, and as negative control, GST alone, and tested their ability to promote capillary array formation in primary HUVEC cultures in the presence of the neprilysin inhibitors phosphoramidon (Fig. 3*C*, *PPA*) and CGS24592 (data not shown). Recombinant and full-length GST-FGF-2 protein promoted similar amounts of array formation. However, neither the 1–135 nor the 136–155 FGF-2 cleavage products demonstrated any biologic activity in this assay.

To establish that neprilysin anti-angiogenic activity is a direct consequence of FGF-2 cleavage, we examined whether cleavage of FGF-2 abrogated its ability to signal through the fibroblast growth factor receptor. Upon engaging FGF-2, FGF receptor undergoes dimerization and autophosphorylation and then signals by way of the mitogen-activated protein kinase pathway resulting in ERK phosphorylation (28). Therefore, we first assessed rNEP inhibition of FGF-2 signaling by blotting HUVEC lysates for phosphorylated ERK and total ERK prepared following treatment with either FGF-2 (100 ng/ml) alone or FGF-2 preincubated with rNEP. As shown in Fig. 4*A*, rNEP treatment decreased FGF-2-induced ERK phosphorylation by ~50%. As a complementary approach, we next examined the effect of neprilysin inhibition on ERK phosphorylation follow-

FIGURE 2. **Neprilysin enzymatic activity cleaves FGF-2 protein.** *A*, basic FGF or VEGF was incubated with or without rNEP for 1 h at 25 °C in 100 mM Tris-HCl, pH 7.6, and the samples separated by 14% SDS-PAGE. *Lane 1*, 12.5 μM FGF-2 + 1 μM rNEP; *lane 2*, 12.5 μM FGF-2 alone; *lane 3*, 12.5 μM VEGF alone; *lane 4*, 12.5 μM VEGF + 1 μM rNEP. Note faster migration of FGF-2 protein treated with rNEP (*arrow*). *B*, 12.5 μM FGF-2 was incubated with or without rNEP and the neprilysin inhibitor CGS24592 for 1 h at 25 °C and the samples separated by 14% SDS-PAGE. *Lane 1*, Me_2SO vehicle (control); *lane 2*, 3 μM CGS24592; *lane 3*, 1 μM rNEP + 12.5 μM FGF-2; *lane 4*, 1 μM rNEP + 12.5 μM FGF-2 + 3 μM CGS24592. Note that the addition of CGS24592 blocks the faster migration of FGF-2 protein treated with rNEP (*lane 4* compared with *lane 3*). *C*, lysates from TSU-Pr1-derived WT5 and M22 cells cultured in tetracycline-free medium for 48 h containing 500 μg of total protein were subjected to immunoprecipitation with J5 antibody and incubated with 100 ng of FGF-2 for 4 h at 37 °C. Samples were analyzed by SDS-PAGE and Western blotted for both FGF-2 and neprilysin. Note the increased electrophoretic mobility seen with wild-type neprilysin (*WT5*), but not enzymatically deficient neprilysin (*M22*). *D*, FGF-2 (12 μM) and neprilysin (400 nM) were incubated in 50 mM Hepes, pH 7.4, 100 mM NaCl and aliquots removed at the various times (1–230 min), quenched with SDS sample buffer, and analyzed by SDS-PAGE. Coomassie-stained intact FGF-2 (*upper arrow on right*) was then quantified densitometrically (NIH ImageJ software) and expressed graphically as the percentage of intact FGF-2, with 100% defined as the intensity of the intact FGF-2 band at time 0, just prior to addition of rNEP. *E*, recombinant neprilysin was incubated with FGF-2 with (*upper panel*) or without (*lower panel*) CGS24592 and analyzed by MALDI-TOF mass spectrometry. Note the presence of a 2019-Da band, which corresponds to amino acids 136–155 of the FGF-2 protein in the absence of CGS24592. *F*, crystal structure of the 155-amino acid form of recombinant FGF-2 (Protein Data Bank accession code 1BFF from Ref. 23). The neprilysin cleavage site is *highlighted*. *G*, fibroblast growth factor-2, rNEP, and heparin were incubated for 1 h at 25 °C in 100 mM Tris-HCl, pH 7.6, and subjected to 14% SDS-PAGE analysis with Coomassie Blue staining. *Lane 1*, 1 μM rNEP alone; *lane 2*, 12.5 μM FGF-2 + 1 μM rNEP + 12 units/ml heparin; *lane 3*, 12.5 μM FGF-2 + 1 μM rNEP; *lane 4*, 12.5 μM FGF-2 alone. Note heparin inhibits the faster migration of FGF-2 protein treated with rNEP (*lane 2*). *Lanes 1* and *4* are controls.

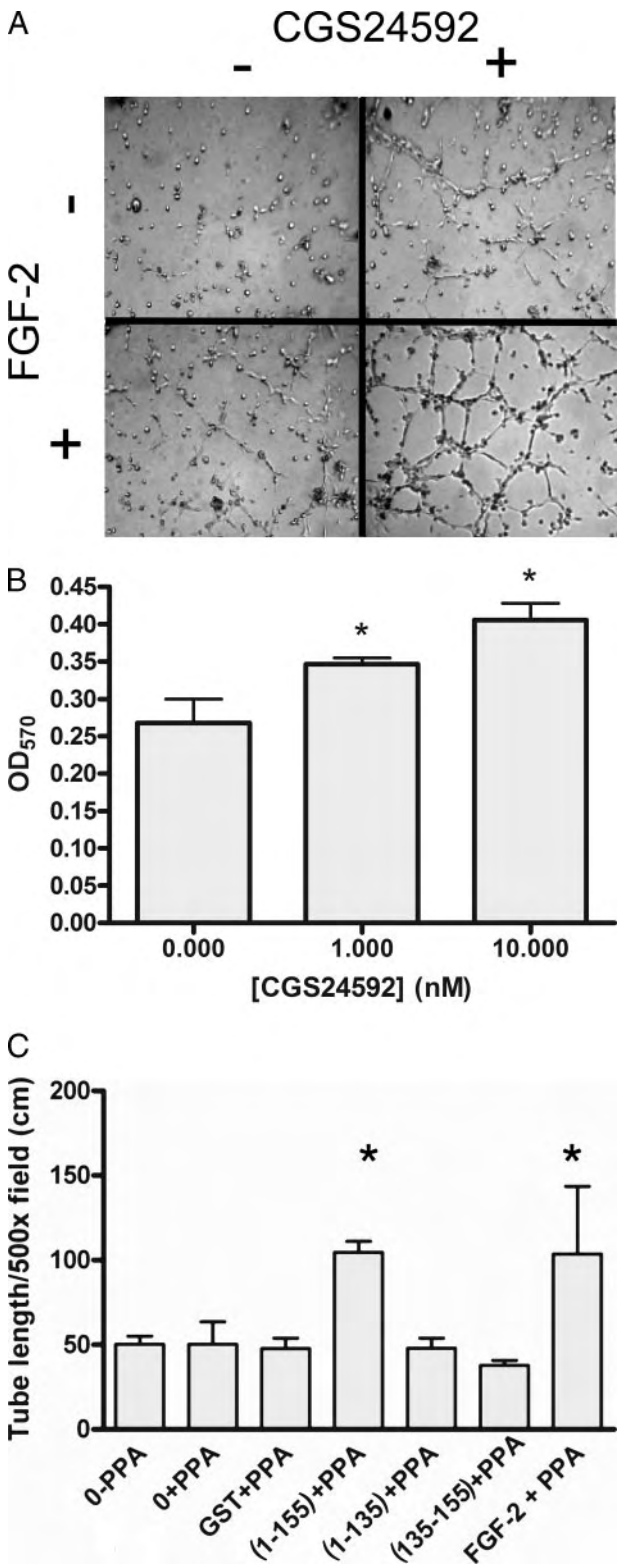

FIGURE 3. **Endogenous neprilysin inhibition enhances FGF-2-induced angiogenesis.** *A*, transduced human bone marrow microvascular endothelial cells were assayed using a Matrigel capillary array formation assay. Cells were plated on growth factor-reduced Matrigel in the presence (+) or absence (−) of CGS24592 (30 nM) for 2 h followed by the addition of FGF-2 (5 ng/ml) for 4 h as indicated. Representative photographs were then taken. *B*, transduced human bone marrow microvascular endothelial cells were incubated with 600 pg/ml FGF-2 in Dulbecco's modified Eagle's medium supplemented with 1% FCS and increasing concentrations of CGS24592. After 48 h, medium was exchanged with that containing MTT at a concentration of 0.5 mg/ml and incubation continued for 4 more h. Incorporated MTT was liberated with Me_2SO and expressed as $A_{570\ nm}$ (* denotes $p < 0.03$ relative to no CGS24592). Results are representative of two independent experiments with similar results performed in triplicate. *C*, 15,000 HUVEC cells were plated on growth factor-reduced Matrigel in the presence or absence of 30 μM phosphoramidon and the indicated commercially available FGF-2 or GST-FGF-2 fusion protein (included FGF-2 amino acids designated in *parentheses*) added to a final concentration of 50 nM. Array formation was quantified after 18 h by measuring total length of capillary cords formed/×500 field using ImageJ software. Results are representative of three independent experiments with similar results performed in triplicate (* denotes $p < 0.05$ relative to GST control).

ing treatment with a 10-fold lower concentration of FGF-2 (10 ng/ml). At this concentration neither FGF-2 nor inhibition of endogenous neprilysin with CGS24592 resulted in appreciable stimulation of ERK phosphorylation (Fig. 4*B*); however, CGS24592 treatment led to an FGF-2-stimulated increase in ERK phosphorylation.

Next we sought to identify the mechanism, either loss of receptor binding or receptor antagonism, by which FGF-2 cleavage results in its inactivation. This was done by simultaneously examining cell surface binding of FGF-2 cleavage products and their ability to induce ERK phosphorylation. On incubation of GST-FGF-2 fusion proteins with intact HUVEC and tHBMEC, FGF-2 cleavage products but not full-length FGF-2 constructs failed to signal through FGF-R (Fig. 4*C*) and coincidentally failed to bind to cultured vascular endothelial cells (Fig. 4*D*), implying that neprilysin cleavage reduces FGF-2 signaling by rendering FGF-2 incapable of binding cell surface receptor. 10% input standards were included on the right side of Fig.4*D* as controls.

Mutagenesis of the neprilysin cleavage site residues to alanines resulted in decreased neprilysin cleavage, with the double mutant L135A/G136A demonstrating a near complete loss of cleavage by neprilysin (Fig. 5*A*). Consistent with neprilysin normally cleaving N-terminal to a hydrophobic residue, the G136A mutant, which adds hydrophobicity to this position, largely retains its ability to be cleaved by neprilysin. When tested in a Matrigel array formation assay, the neprilysin-resistant L135A/G136A FGF-2 was capable of inducing arrays to an extent comparable with that seen with a 10-fold higher concentration of FGF-2 or with CGS24592 treatment (Fig. 5*B*). Taken together, these data suggest that endogenously expressed neprilysin on vascular endothelial cells regulates FGF-2-induced angiogenesis.

DISCUSSION

Our previous studies have demonstrated that neprilysin possesses multiple properties similar to those of tumor suppressor proteins. These inhibitory effects derive both from neprilysin's catalytic action on peptide substrates and from direct protein-protein interactions between neprilysin's short cytoplasmic domain and lyn kinase, PTEN, and ezrin/radixin/moesin proteins. In the current study, we have demonstrated that neprilysin is capable of cleaving FGF-2, resulting in its inactivation and inhibition of angiogenesis *in vivo*. With a primary sequence of 155 amino acids, FGF-2 is the largest reported neprilysin substrate, indicating that substrate specificity is not restricted to peptides less than 43 amino acids, as previously believed, and raising the possibility that neprilysin may inactivate other large

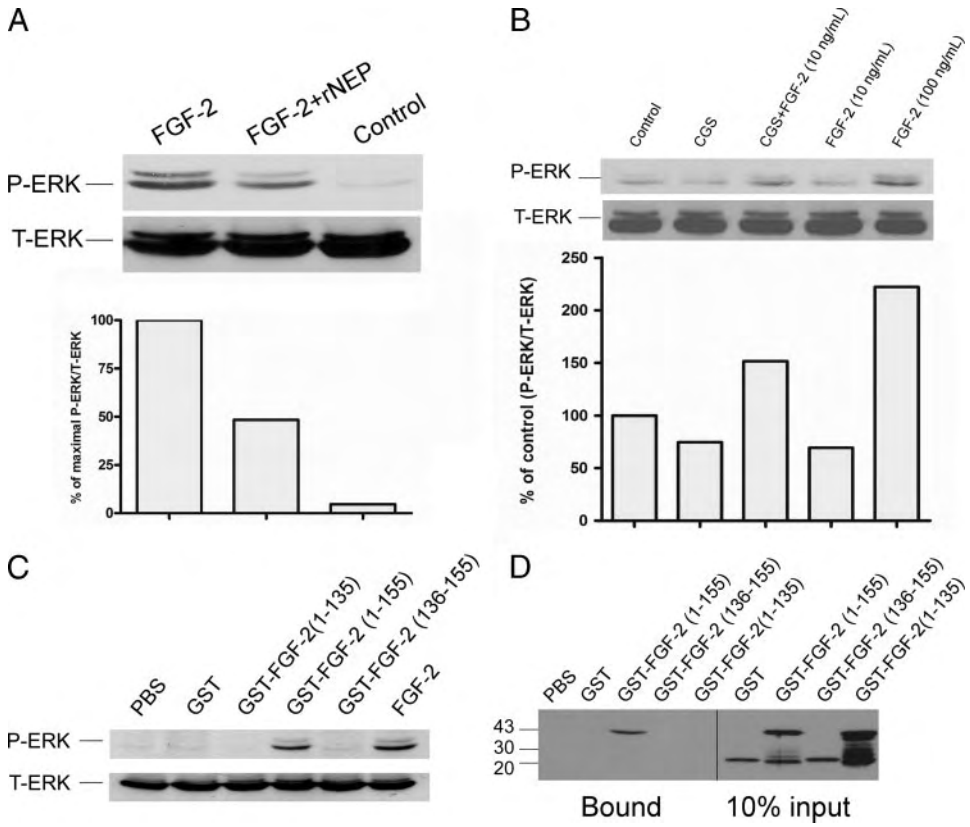

FIGURE 4. **Neprilysin inhibition of FGF-2 signaling through mitogen-activated protein kinase.** *A*, neprilysin attenuation of FGF-2 signaling through ERK. FGF-2 (8 μg/ml) was incubated in the presence or absence of rNEP (60 μg/ml) for 1 h at 25 °C in 100 mM Tris-HCl, pH 7.6, and then added to subconfluent HUVEC monolayers for a FGF-2 concentration of 100 ng/ml, incubated for 20 min, harvested with radioimmune precipitation lysis buffer, and 50 μg of protein subjected to Western blotting analysis using anti-total ERK antibody (*T-ERK*) or anti-phosphorylated ERK antibody (*P-ERK*). As a negative control, buffer alone was used. Results are representative of three independent experiments. The *inset* shows densitometric analysis of the included experiment. *B*, neprilysin inhibition potentiates FGF-2 signaling through ERK. As in *panel A*, FGF-2 and rNEP were incubated and then added to subconfluent HUVEC monolayers that were pretreated with 10 nM CGS24592 or vehicle for 2 h for a final FGF-2 concentration of 10 ng/ml, incubated for 20 min, harvested with radioimmune precipitation lysis buffer, and 50 μg of protein subjected to Western blotting using total ERK (*T-ERK*) or phosphorylated ERK (*P-ERK*) antibodies. The *inset* shows densitometric analysis of the included experiment. *C*, FGF-2 cleavage products are unable to induce mitogen-activated protein kinase phosphorylation. Subconfluent HUVEC monolayers were treated with 5 nM recombinant proteins as indicated for 20 min and washed three times with 2 ml of phosphate-buffered saline. Radioimmune precipitation buffer cell lysates were analyzed for total and phosphorylated ERK as in *panel A*. Recombinant commercially purchased FGF-2 (5 nM) was used as positive control. *D*, testing of FGF-2 cleavage products for binding to intact cells. Lysates from *panel C* were analyzed by SDS-PAGE and blotted with anti-GST antibody. As an in input standard, 10% of each FGF-2 cleavage product included in the experiment was analyzed on the same gel (*four right lanes*).

proteins with sterically permissive tertiary structures. With regard to FGF-2, the external position of the cleavage site permits the generation of a 20-amino acid C-terminal clipped product of FGF-2. These findings also support a novel mechanism by which FGF-2 signaling is attenuated prior to receptor engagement by a cell surface peptidase. Although this mechanism had been proposed previously, given that the C-terminal portion of FGF-2 is cleaved by limited proteolysis *in vitro* with trypsin and chymotrypsin (24), this is the first example of a protease that cleaves FGF-2 resulting in decreased angiogenesis both *in vitro* and *in vivo*.

Cleavage of FGF-2 by neprilysin was rapid *in vitro*, with 50% cleavage occurring in 5–10 min. Although we cannot exclude that neprilysin *in vivo* may be activating another enzyme that in turn cleaves FGF-2, the reaction kinetics using purified proteins are comparable with those observed for other neprilysin substrates; for example, amyloid-β at a 1-μM concentration was observed to be 50% degraded by 150 nM neprilysin in ~5 min (29).

Regulation of the interaction between neprilysin and FGF-2 likely occurs through the actions of extracellular matrix and cell surface HSPG, as suggested by the ability of heparin to protect FGF-2 from cleavage by neprilysin. The putative neprilysin cleavage site is one of the sites where heparanoids are reported to complex with FGF-2 (26), potentially explaining why heparin binding prevents FGF-2 from neprilysin cleavage. Heparan sulfate proteoglycan augments FGF signaling by interacting with both FGF-2 and its receptors, with evidence emerging that FGF-2 may signal through HSPG independently of FGF receptors (30). It is possible that augmentation of signaling may be due in part to protecting FGF-2 from proteolytic cleave by neprilysin, resulting in higher local concentrations of FGF-2 and the cell surface. The FGF-2 cleavage products produced by neprilysin do not have any detectable receptor binding activity, but the 1–135 fragment retains binding to heparin (data not shown) and would be predicted to interact with the plasmin substrate fibrinogen (31), both events associated with enhanced angiogenesis (32), raising the possibility that it may modulate the FGF-2 activity. Likewise, it is possible that the 20-amino acid fragment may possess some as yet undetermined biologic activity and that neprilysin functions to release this product similar to how the neprilysin homologue endothelin-converting enzyme 1 cleaves proendothelin to form the biologically active endothelin-1 (33).

Fibroblast growth factor-2 has been studied extensively in prostate cancer. Of note, neprilysin-expressing LNCaP cells do not produce measurable amounts of FGF-2, in contrast to non-neprilysin-expressing, androgen-independent PC-3 and DU-145 cells (34). Fibroblast growth factor-2 is highly expressed in prostate cancer tissues (35–37), and expression correlates with neovascularization in prostate cancer tissue specimens (38). Patients with prostate cancer have significantly elevated serum FGF-2 levels compared with healthy controls that increase on progression to androgen-independent disease (35). Importantly, androgen-independent prostate cancer is frequently accompanied by loss of tumor cell

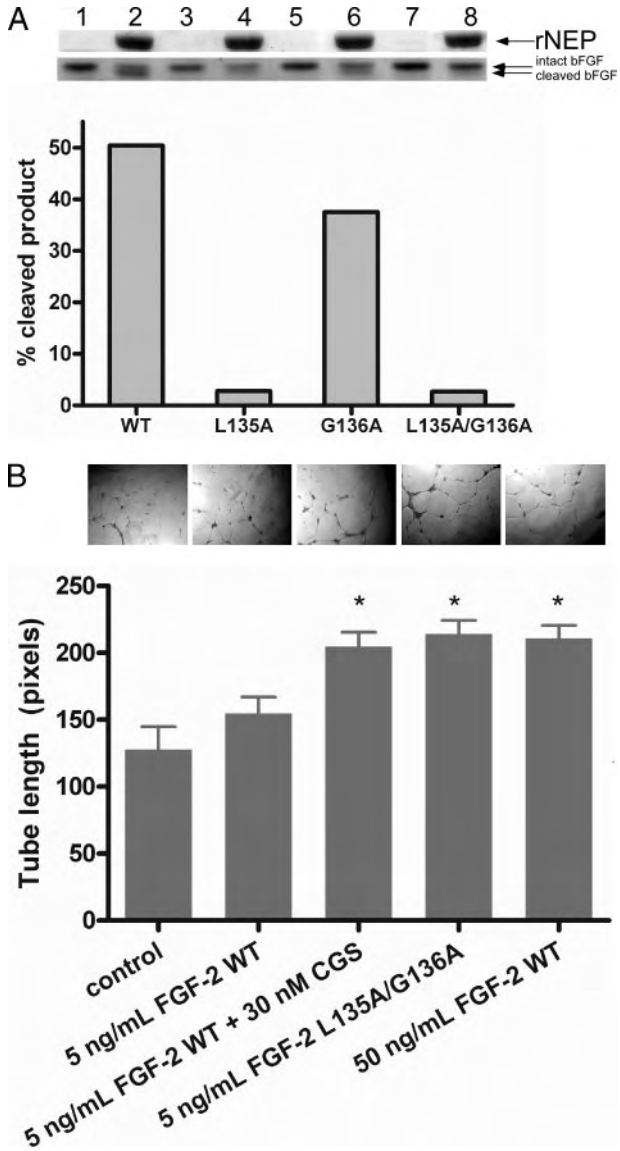

FIGURE 5. **Mutagenesis of the putative neprilysin cleavage site results in abrogation of cleavage and increases FGF-2 potency.** *A*, 1 μg each of wild-type FGF-2 (*lanes 1–2*) and the FGF-2 mutants L135A (*lanes 3–4*), G136A (*lanes 5–6*), and L135A/G136A (*lanes 7–8*) was incubated with 2 μg of rNEP (*even-numbered lanes*) or vehicle (*odd-numbered lanes*) at 25 °C for 12 h in a final volume of 25 μl of 100 mM Tris-HCl, pH 7.2, and subjected to SDS-PAGE analysis. A lower band corresponding to the major cleavage product is observed for wild-type FGF-2 reaction and in varying degrees for the FGF-2 mutants. *Below* is the densitometric analysis (ImageJ software) for each cleavage product expressed as percentage of total FGF-2 (intact + cleaved band) and corrected by subtracting the corresponding pixels obtained in the absence of neprilysin. These data are representative of three individual experiments with similar results. *B*, 15,000 HUVEC cells were plated on growth factor-reduced Matrigel in the presence or absence of 30 nM CGS 24592 and the indicated FGF-2 protein (5–50 ng/ml). Array formation was quantified after 18 h by measuring total length of capillary cords formed/×500 field in five different fields using ImageJ software. Results are representative of three independent experiments with similar results performed in duplicate (*, $p < 0.01$ relative to control and wild-type FGF-2).

neprilysin expression (1), and therefore increased serum FGF-2 in these patients may be explained by our findings. Introduction of FGF-2 into prostate epithelial cells induces a neoplastic phenotype (39), and a recent study showed that FGF-2-mediated angiogenesis promotes tumor progression in the TRAMP animal model of prostate cancer (40).

Neprilysin may possess anti-angiogenic properties in addition to cleaving FGF-2. Neuropeptide substrates of neprilysin implicated in prostate cancer progression such as endothelin-1 (41) and bombesin (42) are capable of inducing FGF-2 as well as VEGF expression. Furthermore, neprilysin stabilizes PTEN protein (7), resulting in reduced levels of phosphorylated Akt, known to induce VEGF expression in vascular endothelial cells (43). Thus, neprilysin appears capable of negatively regulating angiogenesis via multiple signaling pathways.

Our findings implicate the enzymatic activity of neprilysin as anti-angiogenic and may be therapeutically applicable beyond malignant neoangiogenesis. Neprilysin levels are reported to be elevated in diabetic ulcers (44), raising the possibility that impaired wound healing in diabetic patients may result in part from the inhibitory effect of neprilysin on FGF-2. Use of a neprilysin inhibitor administered topically in diabetics in conjunction with recombinant FGF-2 potentially would represent a novel therapeutic approach in these patients. Alternatively, the use of a neprilysin-resistant form of FGF-2 could circumvent the need for a neprilysin inhibitor and provide a novel therapy to target ischemia, where robust angiogenesis is required. Neprilysin loss has also been implicated in the pathogenesis of Alzheimer disease, where its substrate β-amyloid is increased (45). FGF-2 levels are also elevated in amyloid plaques in association with HSPG in the affected brain relative to control, a phenomenon that may be explained by this study (46).

In summary, our studies identify the cell surface peptidase neprilysin as a protease that cleaves and inactivates FGF-2. In addition to inhibiting cell growth and migration via multiple mechanisms, including neuropeptide inactivation and protein-protein interactions, neprilysin functions to inhibit FGF-2-mediated angiogenesis. As an anti-angiogenic protein, neprilysin fulfills a previously unrecognized novel tumor-suppressive function.

Acknowledgments—We thank Anna Awdankiewicz and Daniel Navarro for technical assistance and Heather Orkin for secretarial support.

REFERENCES

1. Papandreou, C. N., Usmani, B., Geng, Y., Bogenrieder, T., Freeman, R., Wilk, S., Finstad, C. L., Reuter, V. E., Powell, C. T., Scheinberg, D., Magill, C., Scher, H. I., Albino, A. P., and Nanus, D. M. (1998) *Nat. Med.* **4,** 50–57
2. Osman, I., Yee, H., Taneja, S. S., Levinson, B., Zeleniuch-Jacquotte, A., Chang, C., Nobert, C., and Nanus, D. M. (2004) *Clin. Cancer Res.* **10,** Pt. 1, 4096–4100
3. Nanus, D. M. (2003) *Clin. Cancer Res.* **9,** 6307–6309
4. Sumitomo, M., Milowsky, M. I., Shen, R., Navarro, D., Dai, J., Asano, T., Hayakawa, M., and Nanus, D. M. (2001) *Cancer Res.* **61,** 3294–3298
5. Sumitomo, M., Shen, R., Walburg, M., Dai, J., Geng, Y., Navarro, D., Boileau, G., Papandreou, C. N., Giancotti, F. G., Knudsen, B., and Nanus, D. M. (2000) *J. Clin. Investig.* **106,** 1399–1407
6. Iwase, A., Shen, R., Navarro, D., and Nanus, D. M. (2004) *J. Biol. Chem.* **279,** 11898–11905
7. Sumitomo, M., Iwase, A., Zheng, R., Navarro, D., Kaminetzky, D., Shen, R., Georgescu, M. M., and Nanus, D. M. (2004) *Cancer Cell* **5,** 67–78
8. Dai, J., Shen, R., Sumitomo, M., Goldberg, J. S., Geng, Y., Navarro, D., Xu, S., Koutcher, J. A., Garzotto, M., Powell, C. T., and Nanus, D. M. (2001) *Clin. Cancer Res.* **7,** 1370–1377

9. Llorens-Cortes, C., Huang, H., Vicart, P., Gasc, J. M., Paulin, D., and Corvol, P. (1992) *J. Biol. Chem.* **267,** 14012–14018
10. Bagnato, A., and Spinella, F. (2003) *Trends Endocrinol. Metab.* **14,** 44–50
11. Jaffe, E. A., Nachman, R. L., Becker, C. G., and Minick, C. R. (1973) *J. Clin. Investig.* **52,** 2745–2756
12. Schweitzer, K. M., Vicart, P., Delouis, C., Paulin, D., Drager, A. M., Langenhuijsen, M. M., and Weksler, B. B. (1997) *Lab. Investig.* **76,** 25–36
13. Olsen, E., and Mohapatra, S. S. (1992) *Int. Arch. Allergy Immunol.* **98,** 343–348
14. Goodman, O. B., Jr., Krupnick, J. G., Gurevich, V. V., Benovic, J. L., and Keen, J. H. (1997) *J. Biol. Chem.* **272,** 15017–15022
15. Casscells, W., Speir, E., Sasse, J., Klagsbrun, M., Allen, P., Lee, M., Calvo, B., Chiba, M., Haggroth, L., Folkman, J., and Epstein, S. E. (1990) *J. Clin. Investig.* **85,** 433–441
16. Hoffman, A. D., Engelstein, D., Bogenrieder, T., Papandreou, C. N., Steckelman, E., Dave, A., Motzer, R. J., Dmitrovsky, E., Albino, A. P., and Nanus, D. M. (1996) *Clin. Cancer Res.* **2,** 1077–1082
17. Volpert, O. V., Lawler, J., and Bouck, N. P. (1998) *Proc. Natl. Acad. Sci. U. S. A.* **95,** 6343–6348
18. Simantov, R., Febbraio, M., Crombie, R., Asch, A. S., Nachman, R. L., and Silverstein, R. L. (2001) *J. Clin. Investig.* **107,** 45–52
19. Kenny, J. (1993) *Biochem. Soc. Trans.* **21,** Pt. 3, 663–668
20. Howell, S., Nalbantoglu, J., and Crine, P. (1995) *Peptides* **16,** 647–652
21. Maniara, W. M., Cipriano, A., and Powell, M. L. (1998) *J. Chromatogr. B Biomed. Sci. Appl.* **706,** 287–294
22. Abraham, J. A., Whang, J. L., Tumolo, A., Mergia, A., and Fiddes, J. C. (1986) *Cold Spring Harbor Symp. Quant. Biol.* **51,** Pt. 1, 657–668
23. Kastrup, J. S., and Eriksson, E. S. (1997) *Acta Crystallogr. Sect. D Biol. Crystallogr.* **53,** 160–168
24. Sommer, A., and Rifkin, D. B. (1989) *J. Cell Physiol.* **138,** 215–220
25. Kajio, T., Kawahara, K., and Kato, K. (1992) *FEBS Lett.* **306,** 243–246
26. Faham, S., Hileman, R. E., Fromm, J. R., Linhardt, R. J., and Rees, D. C. (1996) *Science* **271,** 1116–1120
27. Graf, K., Koehne, P., Grafe, M., Zhang, M., Auch-Schwelk, W., and Fleck, E. (1995) *Hypertension* **26,** 230–235
28. Nugent, M. A., and Iozzo, R. V. (2000) *Int. J. Biochem. Cell Biol.* **32,** 115–120
29. Leissring, M. A., Lu, A., Condron, M. M., Teplow, D. B., Stein, R. L., Farris, W., and Selkoe, D. J. (2003) *J. Biol. Chem.* **278,** 37314–37320
30. Chua, C. C., Rahimi, N., Forsten-Williams, K., and Nugent, M. A. (2004) *Circ. Res.* **94,** 316–323
31. Peng, H., Sahni, A., Fay, P., Bellum, S., Prudovsky, I., Maciag, T., and Francis, C. W. (2004) *Blood* **103,** 2114–2120
32. Sahni, A., Khorana, A. A., Baggs, R. B., Peng, H., and Francis, C. W. (2006) *Blood* **107,** 126–131
33. Xu, D., Emoto, N., Giaid, A., Slaughter, C., Kaw, S., deWit, D., and Yanagisawa, M. (1994) *Cell* **78,** 473–485
34. Nakamoto, T., Chang, C. S., Li, A. K., and Chodak, G. W. (1992) *Cancer Res.* **52,** 571–577
35. Cronauer, M. V., Schulz, W. A., Seifert, H. H., Ackermann, R., and Burchardt, M. (2003) *Eur. Urol.* **43,** 309–319
36. Dorkin, T. J., Robinson, M. C., Marsh, C., Neal, D. E., and Leung, H. Y. (1999) *J. Pathol.* **189,** 564–569
37. Giri, D., Ropiquet, F., and Ittmann, M. (1999) *Clin. Cancer Res.* **5,** 1063–1071
38. Shih, S. J., Dall'Era, M. A., Westphal, J. R., Yang, J., Sweep, C. G., Gandour-Edwards, R., and Evans, C. P. (2003) *Prostate Cancer Prostatic Dis.* **6,** 131–137
39. Ropiquet, F., Berthon, P., Villette, J. M., Le Brun, G., Maitland, N. J., Cussenot, O., and Fiet, J. (1997) *Int. J. Cancer* **72,** 543–547
40. Polnaszek, N., Kwabi-Addo, B., Peterson, L. E., Ozen, M., Greenberg, N. M., Ortega, S., Basilico, C., and Ittmann, M. (2003) *Cancer Res.* **63,** 5754–5760
41. Peifley, K. A., and Winkles, J. A. (1998) *Biochem. Biophys. Res. Commun.* **242,** 202–208
42. Bajo, A. M., Schally, A. V., Groot, K., and Szepeshazi, K. (2004) *Br. J. Cancer* **90,** 245–252
43. Jiang, B. H., Zheng, J. Z., Aoki, M., and Vogt, P. K. (2000) *Proc. Natl. Acad. Sci. U. S. A.* **97,** 1749–1753
44. Antezana, M., Sullivan, S., Usui, M., Gibran, N., Spenny, M., Larsen, J., Ansel, J., Bunnett, N., and Olerud, J. (2002) *J. Investig. Dermatol.* **119,** 1400–1404
45. Carpentier, M., Robitaille, Y., DesGroseillers, L., Boileau, G., and Marcinkiewicz, M. (2002) *J. Neuropathol. Exp. Neurol.* **61,** 849–856
46. Cummings, B. J., Su, J. H., and Cotman, C. W. (1993) *Exp. Neurol.* **124,** 315–325

Prostate Cancer and Prostatic Diseases (2007), 1–9

1365-7852/07 $30.00
www.nature.com/pcan

ORIGINAL ARTICLE

Neutral endopeptidase inhibits prostate cancer tumorigenesis by reducing FGF-2-mediated angiogenesis

A Horiguchi[1], DYT Chen[2], OB Goodman Jr[1,3], R Zheng[1,3], R Shen[1], H Guan[4], LB Hersh[4] and DM Nanus[1,3]

[1]*Urologic Oncology Research Laboratory, Department of Urology, Weill Medical College of Cornell University, New York, NY, USA;* [2]*Section of Urologic Oncology, Department of Surgical Oncology, Fox Chase Cancer Center, Philadelphia, PA, USA;* [3]*Division of Hematology and Medical Oncology, Department of Medicine, Weill Medical College of Cornell University, New York, NY, USA and* [4]*Department of Molecular and Cellular Biochemistry, University of Kentucky College of Medicine, Lexington, KY, USA*

Neutral endopeptidase (NEP) is a cell surface peptidase that catalytically inactivates a variety of physiologically active peptides including basic fibroblast growth factor (FGF-2). We investigated the effect of using lentivirus to overexpress NEP in NEP-deficient DU145 prostate cancer cells. Third-generation lentiviral vectors encoding wild-type NEP (L-NEP), catalytically inactive mutant NEP (L-NEPmu), and green fluorescent protein (L-GFP) were stably introduced into DU145 cells. FGF-2 levels in cell culture supernatants decreased by 80% in L-NEP-infected DU145 cells compared to cells infected with L-NEPmu or L-GFP ($P<0.05$) while levels of other angiogenic factors were not altered. *In vitro* tubulogenesis of human vascular endothelial cells induced by conditioned media from DU145 cells infected with L-NEP was significantly reduced compared with that from DU145 cells infected with L-GFP ($P<0.05$). Tumor xenografts from L-NEP-infected DU145 cells were significantly smaller compared to control cell xenografts and vascularity within these tumors was decreased ($P<0.05$). Our data suggest that stable expression of NEP in DU145 cells inhibits prostate cancer tumorigenicity by inhibiting angiogenesis, with a probable mechanism being proteolytic inactivation of FGF-2.
Prostate Cancer and Prostatic Diseases advance online publication, 12 June 2007; doi:10.1038/sj.pcan.4500984

Keywords: angiogenesis; basic fibroblast growth factor; lentivirus; neutral endopeptidase

Introduction

Neutral endopeptidase (NEP, neprilysin, CD10) is a 90–110 kDa type II integral membrane protein member of the M13 family of zinc peptidases, possessing an extracellular C terminus that contains an active catalytic domain that cleaves peptide bonds on the amino side of hydrophobic amino acids.[1,2] NEP inactivates multiple physiologically active peptides, including atrial natriuretic factor, substance P, bradykinin, oxytocin, Leu- and Met-enkephalins, neurotensin, bombesin, endothelin-1 (ET-1), and β-amyloid. We recently reported that basic fibroblast growth factor (FGF-2) is a previously unidentified NEP substrate.[3] NEP catalytically inactivates FGF-2 by cleavage between residues leucine135 and glycine136 resulting in a biologically inactive FGF-2 protein and impairs FGF-2-stimulated angiogenesis.[3]

NEP is normally expressed on a variety of tissues, including prostatic epithelial cells. Expression of NEP is frequently decreased or lost in prostate cancers via hypermethylation of the NEP promoter or following androgen withdrawal.[4–6] Loss of NEP in prostate cancer cell lines results in increased peptide-mediated cell growth, cell migration and invasion, and ligand-independent activation of the insulin-like growth factor-1 receptor leading to Akt phosphorylation.[4,7,8] Loss of NEP *in vivo* in primary prostate cancers correlates with increased Akt phosphorylation, and predicts biochemical relapse in patients who have undergone radical prostatectomy.[6,9] Together, these studies suggest that NEP loss contributes to prostate cancer progression.

To assess the antitumor effects of re-expressing NEP, we previously used a tetracycline-repressible system (Tet-off) to regulate NEP expression in TSU-Pr1 cells, which at that time were believed to be of prostate cancer derivation but subsequently were shown to derive from a bladder cancer cell line.[10] In those studies, tetracycline-regulated expression of NEP resulted in inhibition of cell growth, cell migration and tumorigenesis in an orthotopic model of prostate cancer,[4,7,11] indicating that NEP functioned in part as a tumor suppressor. To extend these observations in a prostate cancer cell line model, and to simultaneously assess if NEP could be delivered to prostate cancer cells using a delivery system that would

Correspondence: Dr DM Nanus, Division of Hematology and Medical Oncology, Department of Medicine, Weill Medical College of Cornell University, 525 E. 68th St., ST-359, New York, NY 10021, USA.
E-mail: dnanus@med.cornell.edu
Received 19 February 2007; accepted 3 May 2007

have greater clinical relevance, we examined a lentiviral gene delivery system. Lentiviruses such as human immunodeficiency virus type-1 have been developed for *in vitro* and *in vivo* gene delivery.[12,13] Lentiviral vectors have numerous advantages for gene delivery, including the ability to infect non-dividing cells, long-term transgene expression and absence of induction of host inflammatory and immune responses.[12] Recent studies have begun to examine their utility in cancer gene therapy. Pellinen *et al*.[14] reported a 50–95% lentiviral gene transfer efficiency in studies of 42 tumor cell lines from 10 different human tumor types, and lentiviral-mediated inhibition of cell growth and/or tumor formation in athymic mice have been demonstrated in prostate cancer,[15–18] liver cancer,[19] oral squamous cancer,[20] cervical cancer[21] and melanoma.[19,22] We chose to evaluate the effect of lentiviral vector-mediated NEP transfer in NEP-deficient DU145 cells. We report here that lentivirus is an effective tool for NEP transfer into prostate cancer cells and results in significant inhibition of tumorigenesis, with a probable mechanism being inhibition of FGF-2-mediated angiogenesis.

Materials and methods

Cells and reagents

The androgen-independent metastatic prostate cancer cell line DU145 was obtained from the American Type Culture Collection (Manassas, VA, USA) and grown in RPMI 1640 medium supplemented with 2 mM glutamine, 1% nonessential amino acids, 100 U/ml streptomycin and penicillin, and 10% fetal calf serum (FCS). Human umbilical vein endothelial cells (HUVEC) were isolated and maintained as described previously.[23] Antibodies used in this study include anti-NEP antibody (NCL-CD10-270, Novocastra Laboratories Ltd, Newcastle upon Tyne, UK), fluorescein isothiocyanate (FITC)-conjugated anti-NEP antibody (J5, Beckman Coulter, Fullerton, CA, USA), anti-phospho-Akt antibody (Ser473) (Cell Signaling Technology Inc., Beverly, MA, USA), anti-Akt antibody (Cell Signaling Technology), anti-phospho-FAK antibody (Tyr397, Biosource, Camarillo, CA, USA), anti-FAK antibody (C-20, Santa-Cruz Biotechnology Inc., Santa Cruz, CA, USA), anti-phosphatase and tensin homolog (PTEN) antibody (A2B1, Santa-Cruz Biotechnology Inc.) and anti-alpha smooth muscle actin (αSMA) antibody (Dako Cytomation, Carpinteria, CA, USA).

Lentiviral vector production and transduction

A four-plasmid expression system was used to generate third-generation lentiviral vectors by transient transfection as described previously.[12,13] The vector plasmids that expressed green fluorescent protein (L-GFP), wild-type NEP (L-NEP) or enzymatically inactive mutant NEP (L-NEPmu) driven by the human cytomegalovirus promoter were constructed as described.[12,13] The lentiviral vector titers were estimated by flow cytometric analyses (fluorescence-activated cell sorting (FACS)) as described previously.[13] DU145 cells were transduced with L-GFP, L-NEP or L-NEPmu at the indicated multiplicity of infection (MOI) in the presence of 6 μg/ml polybrene (Sigma-Aldrich, St Louis, MO, USA) for 72 h.

NEP enzyme activity assay

NEP-specific enzyme activities in the transduced cells and tissues were assessed as described using Suc-Ala-Ala-Phe-pNA (Bachem Bioscience Inc., Philadelphia, PA, USA) as substrate.[24] Specific activities were expressed as picomoles per microgram of protein per minute and represent an average of two separate measurements performed in duplicate.

Cell proliferation assay

DU145 cells were plated in six-well plates (5×10^3/well in triplicate) overnight and then infected with lentiviral vectors. The total cell number was counted at the indicated time. Results were expressed as an average of two separate measurements performed in triplicate.

Matrigel invasion assay

Invasion was assessed using Matrigel-coated Biocoat cell culture inserts (BD Biosciences, San Jose, CA, USA) with 8-μm pores in 24 wells, as described previously.[25] Briefly, a suspension of 5×10^4 cells in serum-free RPMI were added to each insert and RPMI supplemented with 10% FCS were added to the bottom of each well. The plates were incubated for 24 h at 37°C. Inserts were fixed and stained with Diff-Quik Stain Set (Dade Behring Inc., Deerfield, IL, USA), and cells invading through each of the Matrigel-coated transwell inserts were counted at $\times 40$ magnification. Results were expressed as an average of two separate measurements performed in triplicate.

Immunoblotting and immunoprecipitation

Immunoblotting and immunoprecipitation were carried out as described previously.[26,27] For immunoprecipitations, 600 μg of precleared total cell lysates were incubated with 2 μg of anti-PTEN antibody for 2 h at 4°C and 40 μl of protein G-Sepharose beads (Amersham Pharmacia Biotech, Piscataway, NJ, USA) for 1 h. Protein complexes were separated by sodium dodecyl sulfate polyacrylamide gel electrophoresis and detected with the appropriate antibody.

Determination of growth factors secretion

Stably transduced DU145 cells were plated at 1×10^4 cells/well in six-well plates in RPMI 1640 containing 10% FCS for 24 h, and then were washed with serum-free medium and cultured for an additional 48 h in serum-free medium. The medium was collected and centrifuged. The levels of growth factors in the supernatants were analyzed using a Beadlyte growth factor detection kit (Upstate Biotechnology, Lake Placid, NY, USA). Results were expressed as an average of two separate measurements performed in triplicate.

Real time reverse transcription-PCR

Total RNA was extracted with Trizol (Invitrogen, Carlsbad, CA, USA) following the manufacturer's instructions. One microgram of total RNA was then reverse-transcribed into cDNA using Superscript First-Strand Synthesis system for reverse transcription PCR (RT-PCR; Invitrogen). Real-time RT-PCR was performed using SYBR Green PCR Master Mix with the ABI Prism

7700 Sequence Detector (Applied Biosystems, Foster City, CA, USA) following the manufacturer's instructions. The PCR primer pair used for FGF-2 was described previously.[28] Results were obtained as an average of measurements performed in triplicate.

HUVEC tube formation assay
Transduced DU145 cells were plated at 1×10^4 cells/well in six-well plates in RPMI 1640 containing 10% FCS for 24 h, and then were washed with serum-free medium and cultured for an additional 48 h in serum-free medium. The medium was collected and centrifuged and used as conditioned media. A 96-well plate was coated with 10 mg/ml of growth factor-reduced matrigel (BD Biosciences) at 37°C for 30 min. HUVECs (1.5×10^4 cells/well) were cultured in a 96-well plate coated with matrigel in conditioned media from transduced DU145 cells for 18 h and the total length of tube-like structures of five randomly chosen microscopic fields was measured by Image J software.

Assessment of tumorigenicity of transduced DU145 cells
Transduced DU145 cells (5×10^6 cells) were inoculated subcutaneously into the flanks of nude mice (Taconic, Hudson, NY, USA). The tumor volumes were monitored every 3 or 4 days. Tumor volume was estimated by using the formula volume = width^2 × length × 0.52 in mm^3. At day 29, the mice were killed, and the tumors were removed for further experiments. Animal experiments were reviewed and approved by the Institutional Animal Care and Use Committee.

Immunohistochemistry
Immunohistochemistry was performed using DAKO EnVision+ system HRP (DAKO) according to the manufacturer's instruction. Vascularity in each tumor specimen was estimated using anti-αSMA antibody (DAKO). Three areas of vascularization were selected under a light microscope with a 200-fold magnification and the mean count of those areas was recorded for each tumor section.

Statistical analysis
All analyses were performed using StatView 5.0 (SAS Institute Inc., Cary, NC, USA). Results were expressed as the mean ± s.e. for three independent measurements in two separate experiments. Analysis of variance was used for analyses of continuous data followed by Fisher's protected least significant difference for *post hoc* analyses. Differences with a $P < 0.05$ were determined as statistically significant

Results

Lentiviral transduction of wild-type and enzymatically inactive mutant NEP
Lentivirus vectors expressing wild-type NEP (L-NEP), NEP with a point mutation in the extracellular catalytic domain rending the protein enzymatically inactive (L-NEPmu) or control GFP protein (L-GFP) were each introduced into DU145 cells to examine the efficiency of lentiviral transduction in PC cells (Figure 1A). As shown in Figure 1B, NEP protein expressed by L-NEP and L-NEPmu were detected by immunoblot analysis at an MOI of 10, 20 and 50 in a dose-dependent fashion. L-GFP expression was confirmed using an immunofluorescent microscope (Figure 1C, panel a). Lentiviral-mediated NEP expression by L-NEP and L-NEPmu were also detected by immunocytochemistry with a FITC-conjugated anti-NEP antibody under immunofluorescent microscope. In DU-NEP and DU-NEPmu cells, clear membranous and perinuclear staining for NEP was observed (Figure 1C, panels b and c, respectively). To confirm cell surface expression, NEP was analyzed by FACS at MOI 1–50, which showed that 80.3 ± 2.5 and 80.4 ± 2.2% of DU-NEP and DU-NEPmu cells were positive for NEP at MOI 50, while 99.4 ± 0.2 % of DU-GFP cells were positive for GFP at MOI 50 (Figure 1D). To confirm that DU-NEP, but not DU-GFP or DU-NEPmu, expressed biologically active NEP, we next performed NEP-specific enzyme assays. At MOI 50, DU-NEP cells possessed a specific activity of 96.5 ± 10.2 pmol/μg/min, whereas DU-NEPmu and DU-GFP cells produced only 1.0 ± 0.4 and 1.3 ± 0.7 pmol/μg/min, respectively ($P < 0.001$ vs DU-GFP) (Figure 1E). Based on these results, we concluded that lentivirus vector could efficiently transduce NEP into DU145 cells and only L-NEP could generate catalytically active NEP.

Infection of DU145 cells with lentivirus vectors at a higher MOI resulted in virus-induced nonspecific cytotoxicity (data not shown). Therefore, we used lentivirus vector at MOI 50 for further studies. Cells were amplified and stored at −80°C following infection and cells of similar passage were used in experiments described below. No difference in protein expression or enzyme activity of NEP and GFP was detected between freshly infected and stored cells.

Lentiviral NEP expression effects on DU145 cells
We previously reported that the re-expression of wild-type NEP using a tetracycline repressive system in NEP-deficient TSU-Pr1 cells resulting in NEP enzyme activity of 1180 pmol/μg/min, a 10-fold higher specific activity than that achieved in DU145 cells infected with L-NEP. Expression of NEP in TSU-Pr1 cells resulted in significant inhibition of cell growth and cell invasion.[4,7,11,27] In contrast, cell proliferation or cell invasion in DU-NEP cells was no different than DU-NEPmu or control DU-GFP cells (Figure 2a, b). NEP has been shown to inhibit Akt phosphorylation.[7] Bombesin-induced Akt phosphorylation was only partially, but not completely, inhibited in DU-NEP cells (Figure 2c). Expression of wild-type NEP can also inhibit peptide-mediated FAK phosphorylation in TSU-Pr1 cells.[27] As shown in Figure 2d, expression of NEP in DU-NEP cells did not alter FAK phosphorylation in DU145 cells. Finally, the NEP protein physically associates with and stabilizes the PTEN tumor suppressor protein via a direct protein–protein interaction between the NEP cytoplasmic domain and a negatively charged phosphorylation site in PTEN C terminus.[26] Immunoprecipitation experiments showed that NEP and PTEN did co-associate in both DU-NEP and DU-NEPmu cells, both of which possess intact cytoplasmic NEP domains but not DU-GFP cells (Figure 2e). Together, these data show that lentivirus-mediated NEP expression in DU145 cells resulted in moderate levels of NEP

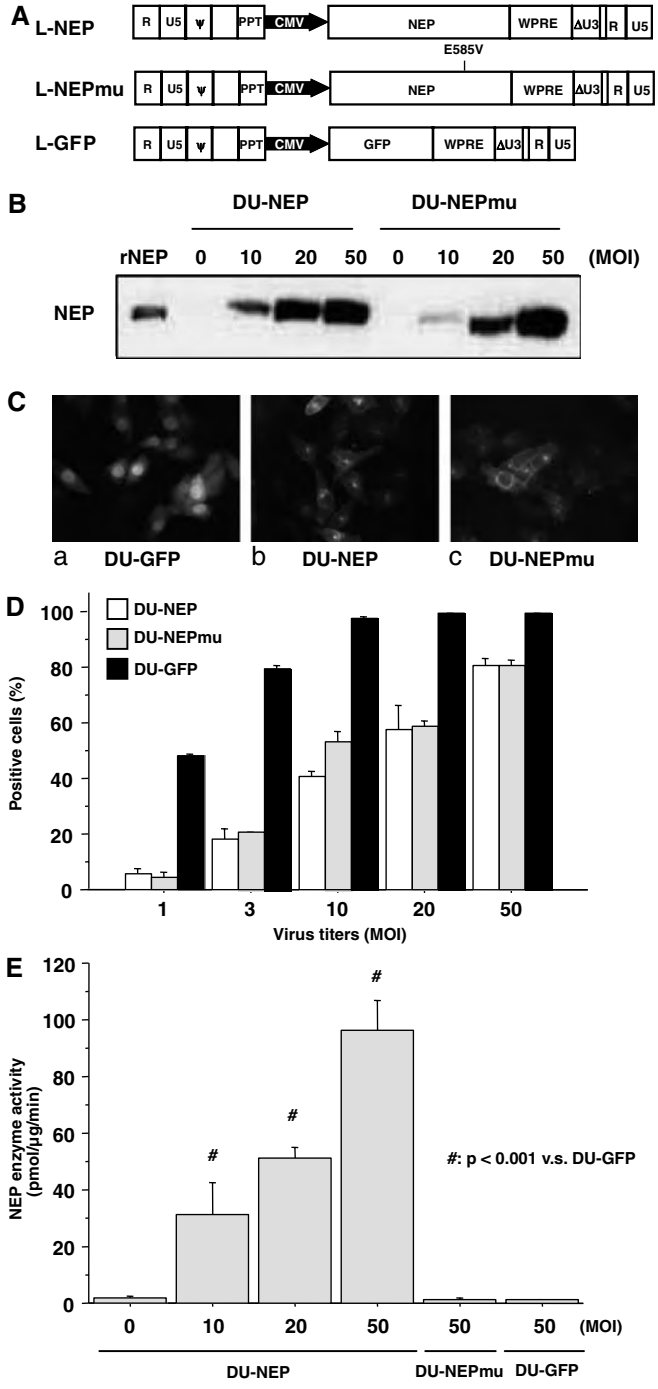

Figure 1 Transduction of DU145 cells with lentiviral vectors. (**A**) Schematic representation of the vectors encoding wild-type NEP (L-NEP), point mutant of NEP (E585V) showing enzymatically inactive NEP (L-NEPmu) and green fluorescent protein (L-GFP) driven by the CMV promoter.[13] (**B**) Total cell lysates from DU145 cells infected with L-NEP (DU-NEP) or L-NEPmu (DU-NEPmu) for 72 h at the indicated MOIs were prepared and expression of NEP was analyzed by immunoblotting using anti-NEP mouse monoclonal antibody NCL-CD10. Recombinant NEP (rNEP) was used as positive control. (**C**) DU145 cells infected with L-GFP (DU-GFP (a)) showed nuclear and cytoplasmic expression of GFP. DU-NEP (b) and DU-NEPmu (c) cells stained with FITC-conjugated anti-NEP antibody showed membranous and cytoplasmic immunolocalization of NEP. (**D**) To confirm cell surface expression, infected cells were analyzed by FACS in three independent measurements. (**E**) NEP-specific enzyme activities in transduced DU145 cells. Significantly increased enzyme activity was found at MOI 10–50 in DU-NEP cells, but not in DU-GFP or DU-NEPmu cells. $^{\#}P < 0.001$ vs DU-GFP cells. CMV, cytomegalovirus; FACS, fluorescence-activated cell sorting; FITC, fluorescein isothiocyanate; MOI, multiplicity of infection; NEP, neutral endopeptidase.

expression sufficient to associate with PTEN but that the associated enzymatic activity failed to inhibit cell growth or invasion, neuropeptide-induced Akt-phosphorylation or FAK phosphorylation.

Lentiviral NEP expression decreases FGF-2 levels and in vitro *angiogenesis*

DU145 cells release significant amounts of growth factors such as FGF-2 and vascular endothelial growth factor

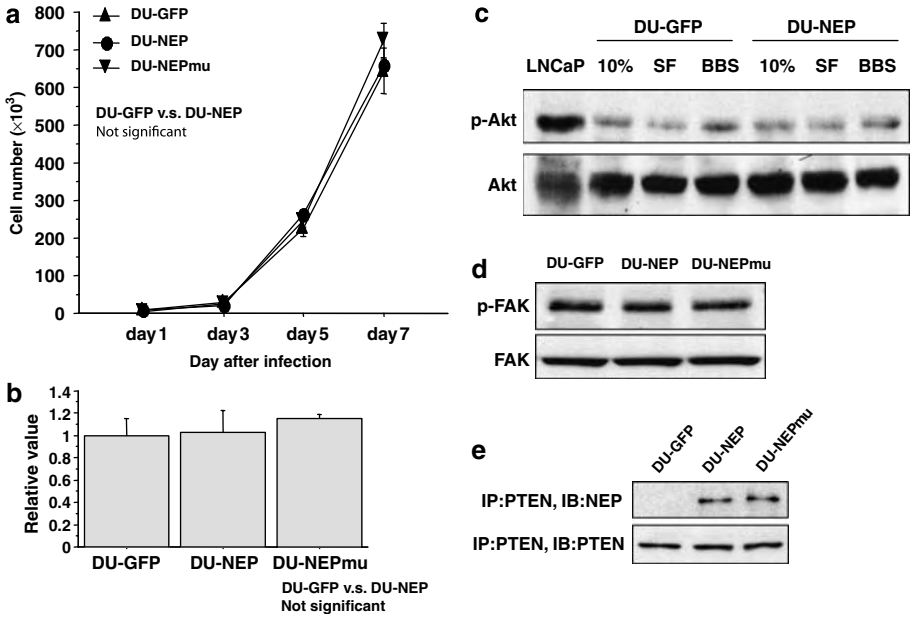

Figure 2 Effect of lentiviral NEP expression on signaling pathways and cell growth and invasiveness of DU145 cells. (**a**) Cell growth curve of transduced DU145 cells. DU-GFP, DU-NEP and DU-NEPmu cells were plated in six-well plates at 5×10^3/well in triplicate and total cell numbers were counted at the indicated times. No significant difference was found among three groups. (**b**) Relative values of the number of cells invading through the Matrigel-coated invasion chamber as compared to DU-GFP cells. (**c**) Lentiviral expression of NEP partially, but not completely, blocked bombesin-induced Akt phosphorylation. DU-GFP and DU-NEP cells were serum-starved and left untreated in serum-free media (SF) or stimulated with 10 nM bombesin for 10 min (BBS) and subjected to immunoblotting. DU-GFP, DU-NEP and LNCaP cells cultured in media with 10% FCS (10%) were used as positive controls for phosphorylated Akt. (**d**) Lentiviral expression of NEP did not inhibit FAK tyrosine phosphorylation. DU-GFP, DU-NEP and DU-NEPmu cells were cultured in media with 10% FCS and subjected to immunoblotting. No difference in FAK phosphorylation was found among three groups. (**e**) Lentiviral wild-type NEP and mutant NEP associate with PTEN tumor suppressor, but not increased PTEN expression. Total cell lysates from transduced cells were immunoprecipitated with anti-PTEN antibody and were blotted to anti-NEP or anti-PTEN antibody (left panel). FAK, focal adhesion kinase; FCS, fetal calf serum; NEP, neutral endopeptidase; PTEN, phosphatase and tensin homolog.

(VEGF) into cell culture supernatants, both of which are potent angiogenic factors.[29,30] Therefore, we measured the concentrations of various pro-angiogenic factors, including FGF-2, VEGF, platelet-derived growth factor (PDGF)-AA, PDGF-AB/BB, epidermal growth factor (EGF) and fms-like tyrosine (FLT-3) ligand in conditioned media from transduced DU145 cells. There were no significant differences in the levels of VEGF, PDGF-AA, PDGF-AB/BB among DU-NEP, DU-NEPmu or DU-GFP cells (Table 1). Production of EGF or FLT-3 ligand could not be detected in any of the conditioned media. However, the level of FGF-2 in the conditioned media from DU-NEP cells (25.6 ± 10.7 pg/ml) was significantly lower than those from DU-GFP (109.0 ± 12.9 pg/ml) or DU-NEPmu cells (102.3 ± 35.8 pg/ml) ($P < 0.05$) (Table 1). To examine whether decreased concentration of FGF-2 in the conditioned media from DU-NEP cells was due to decreased mRNA expression or post-transcriptional modification, we examined FGF-2 mRNA levels in transduced DU145 cells by real-time RT-PCR. There was no significant difference in FGF-2 mRNA levels among transduced DU145 cells (data not shown).

We next examined the effect of lentiviral NEP expression on *in vitro* angiogenesis using a HUVEC tubulogenesis assay. Conditioned media from transduced DU145 cells were applied to HUVEC cells plated and cultured in matrigel and the length of tubular structures measured. The length of tubular structures in HUVEC cultured in conditioned media from DU-NEP cells was significantly shorter than those from DU-GFP or DU-NEPmu cells (48.8 ± 3.3% reduction compared to DU-GFP, $P < 0.05$) (Figure 3A and B). Together, these data show that transduced NEP results in the enzymatic inactivation of FGF-2 secreted into DU-NEP conditioned media, resulting in decreased angiogenesis. Moreover, the level of bFGF production observed in the conditioned media from NEP-deficient cells is sufficient to independently support HUVEC tubulogenesis.

Table 1 The level of growth factor produced by transduced DU145 cells

Growth factor (pg/ml)	*DU-GFP*	*DU-NEP*	*DU-NEPmu*	P-*value*
FGF-2	109.0 (12.9)	25.6 (10.7)	102.3 (35.9)	<0.05[a]
VEGF	758.0 (40.5)	786.7 (55.7)	795.0 (59.8)	NS
PDGF-AA	102.6 (15.7)	138.5 (18.5)	164.8 (25.4)	NS
PDGF-AB/BB	41.4 (12.1)	59.4 (14.7)	67.1 (13.9)	NS
EGF	UD	UD	UD	NS
Flt-3 ligand	UD	UD	UD	NS

Abbreviations: EGF, epidermal growth factor; GFP, green fluorescent protein; NEP, neutral endopeptidase; NS; not significant; UD; undetectable.
Data is shown in mean (s.e.) of triplicate measurements.
[a]DU-NEP vs DU-GFP.

Lentiviral NEP expression suppresses the tumorigenic potential of DU145 xenografts

We next examined the effect of lentiviral NEP expression on tumor formation *in vivo*. DU-NEP cells, DU-NEPmu cells and DU-GFP cells were inoculated into the flank of

athymic mice and tumor volume serially monitored for 29 days. The mean tumor volume of DU-NEP tumors was $465.3 \pm 244.0\,mm^3$, which was significantly smaller than that of control DU-GFP tumors ($1119.9 \pm 154.9\,mm^3$, $P < 0.05$) (Figure 4a). The mean tumor volume of DU-NEPmu tumors ($775.4 \pm 108.0\,mm^3$) was larger than that of DU-NEP tumors, but did not reach statistical significance ($P = 0.0603$) (Figure 4a). The mean value of NEP enzyme activities from protein lysates extracted from DU-NEP tumors was 152.6 ± 26.2 pmol/μg/min, which was significantly higher than those of DU-GFP or DU-NEPmu tumors (24.6 ± 2.05 and 37.4 ± 4.1 pmol/μg/min, respectively, $P < 0.01$) (Figure 4b), suggesting that lentiviral NEP expression was sustained *in vivo*. Because lentiviral NEP expression had no effect on *in vitro* cell growth or invasive capacities of DU145 cells, but significantly inhibited production of FGF-2 and *in vitro* angiogenesis, we hypothesized that decreased angiogenesis reduced tumorigenesis in DU-NEP xenografts. We therefore assessed tumor vascularity by immunohistochemical assessment of smooth muscle actin, a vascular marker. The mean number of vascular structures in DU-NEP xenografts was significantly lower than detected in DU-NEP or DU-NEPmu xenografts ($60.2 \pm 14.5\%$ reduction vs DU-GFP tumor, $P < 0.05$) (Figure 4c). Moreover, the caliber of vessels in DU-NEP tumor was smaller than those in DU-GFP or DU-NEPmu tumors (Figure 4d). These results suggested that the lentiviral NEP inhibition of tumorigenesis of DU145 cells was mediated by the anti-angiogenic effect of NEP, through its ability to cleave and inactivate FGF-2.

Discussion

NEP is a cell-surface peptidase with numerous physiologic functions.[31,32] In recent years, NEP has emerged as an important tumor suppressor gene product. Reduced NEP enzymatic activity facilitates peptide-mediated proliferation by allowing accumulation of higher peptide concentrations at the cell surface, and likely contribute to development or progression of neoplasia. Using prostate cancer as a model, we have demonstrated that the effects of NEP are mediated by its ability to catalytically inactivate substrates such as bombesin and ET-1, but also through direct protein–protein interaction with other proteins such as Lyn kinase (which associates with the p85 subunit of phosphatidylinositol 3-kinase (PI3-K) resulting in NEP-Lyn-PI3-K protein complex), ezrin/radixin/moesin proteins, and the PTEN tumor suppressor protein. Based on these observations, we have explored therapeutic strategies to replace NEP in prostate cancers that are NEP-deficient. Whereas recombinant NEP (rNEP) can inhibit the growth of prostate cancer cells *in vitro*,[4] we were unable to achieve tumor xenograft growth inhibition via intraperitoneal administration of rNEP in mice, possibly related to the inability to reach a sufficient peak serum concentration of rNEP.[11] In the current study, we used lentiviral vectors to deliver NEP to DU145 prostate cancer cells.

Although NEP was successfully and stably introduced into DU145 cells, we did not observe the degree of *in vitro* growth inhibition obtained in prior studies using a tetracycline-regulated system. This may result from the fact that we did not achieve sufficient NEP catalytic

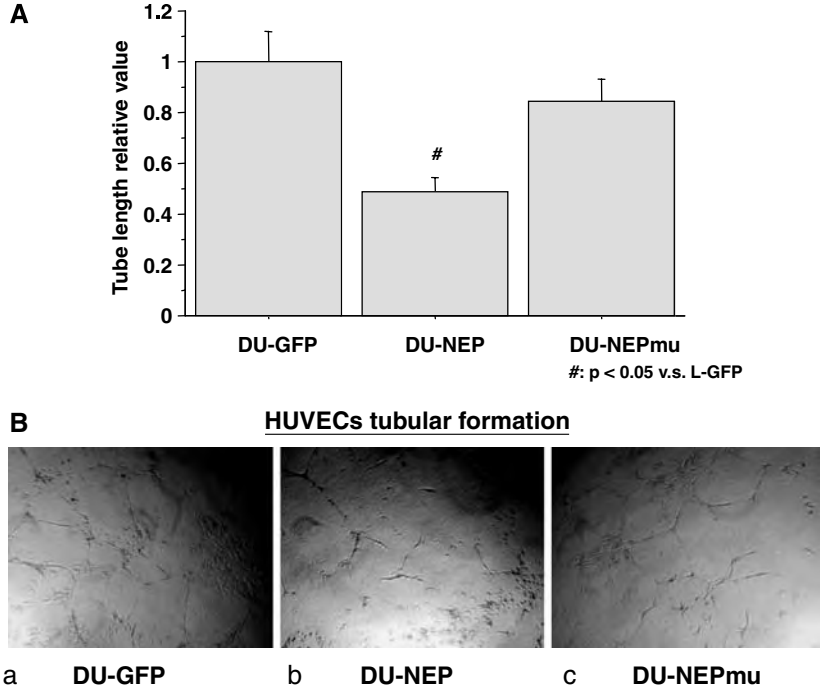

Figure 3 Conditioned media from DU-NEP cells decreased HUVECs tubulogenesis compared to DU-GFP or DU-NEPmu cells. (**A**) Effect of conditioned media from transduced DU145 cells on HUVECs tubular structure formation on Matrigel *in vitro*. HUVECs were cultured with conditioned media from transduced DU145 cells for 18 h on Matrigel basement membrane. Tubular length was quantified in five randomly selected fields. $^{\#}P < 0.05$ vs DU-GFP cells (**B**) Representative photo micrographs ($\times$ 200) of HUVEC tubular formation in conditioned media from DU-GFP (a), DU-NEP (b) and DU-NEPmu (c) cells. GFP, green fluorescent protein; HUVEC, human umbilical vein endothelial cells; NEP, neutral endopeptidase.

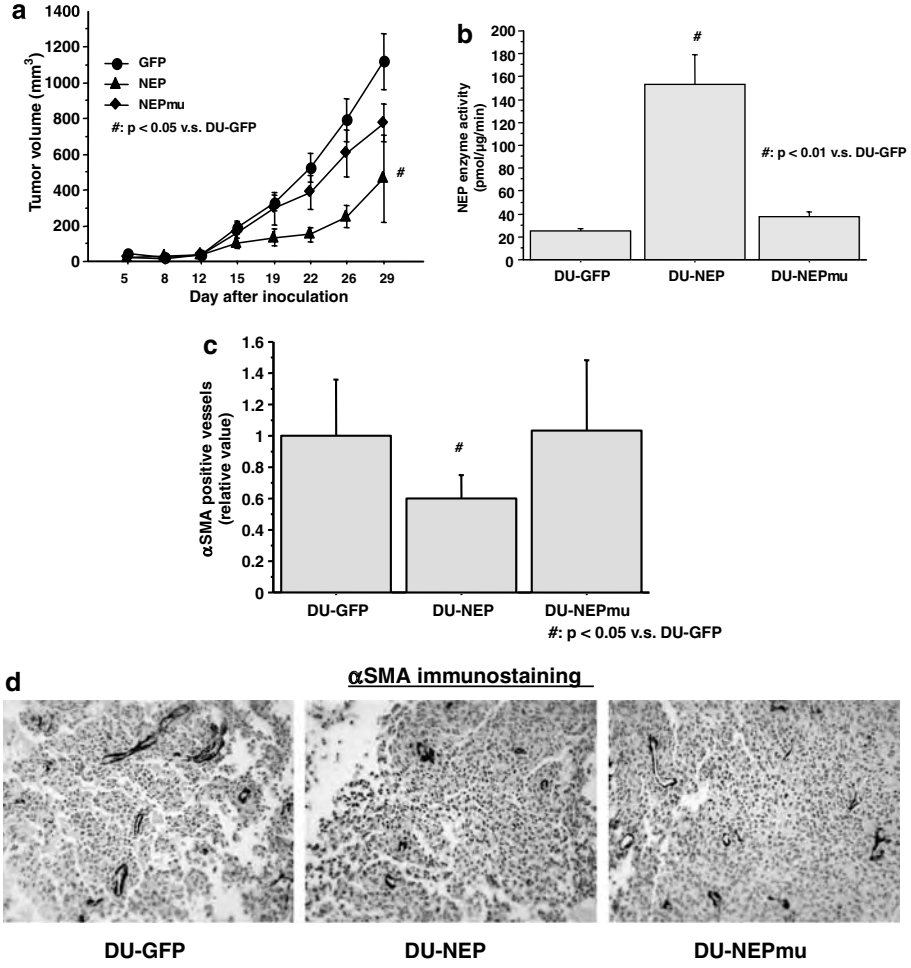

Figure 4 Lentiviral NEP expression inhibited tumorigenesis of DU145 cells with reduced angiogenesis. (**a**) Transduced DU145 cells were inoculated subcutaneously into the flank of nude mice. Tumor volumes were measured every 3 or 4 days until 29 days after inoculation. $^{\#}P<0.05$ vs DU-GFP tumors. ($n=14$ in DU-GFP, $n=7$ in DU-NEP and DU-NEPmu). (**b**) Mean NEP enzyme activities in the established tumors. NEP enzyme activities in DU-NEP tumors were significantly higher than those in DU-GFP, or DU-NEPmu tumors. $^{\#}P<0.01$ vs DU-GFP tumors. (**c**) Relative value of the mean number of αSMA-positive vessels in DU-GFP, DU-NEP and DU-NEPmu tumors. $^{\#}P<0.05$ vs DU-GFP tumors. (**d**) Representative photographs of αSMA immunostaining in DU-GFP, DU-NEP and DU-NEPmu tumors. Note the number and the caliber of αSMA-positive vessels. αSMA, alpha smooth muscle actin; GFP, green fluorescent protein; NEP, neutral endopeptidase.

activity in DU145 cells. Marr *et al*.[13] reported that 293T cells infected with L-NEP at MOI 50 produced an NEP activity of 617 pmol/μg/min, which was approximately sixfold higher than that detected in DU-NEP cells. We previously established TSU-GK27-NEP5 (WT5) cells, which is a stable transfectant with wild-type NEP derived from TSU-Pr1 cells.[4,11] The WT5 cells showed an NEP enzyme activity of 1180 pmol/μg/min and effectively inactivate neuropeptide-induced signals.[4,11,27] Compared to 293T cells infected with L-NEP and WT5 cells, DU-NEP cells showed much lower NEP enzyme activity. The reason for this difference is unclear, although it is possible that expression of higher levels of NEP may be toxic to DU145 cells owing to their dependence on NEP substrates for growth and thus high-expressing cells do not survive in tissue culture.

We recently reported a novel function of NEP as an anti-angiogenic agent by direct proteolytic cleavage of FGF-2 without an effect on VEGF.[3] NEP cleaves FGF-2 between Leu 135 and Gly 136, with the resulting cleavage products lacking angiogenic activity. In the present study, we demonstrated that the concentration of FGF-2, but not VEGF or PDGF, in the conditioned media from DU-NEP cells was significantly lower than conditioned media derived from DU-GFP or DU-NEPmu cells, while no significant difference in the level of FGF-2 mRNA was detected. These results indicate that FGF-2 protein is cleaved by NEP in the extracellular space. Thus, although NEP enzymatic activity in DU-NEP cells was not sufficient to demonstrate an *in vitro* effect, it was sufficient to cleave endogenous FGF-2 produced by DU145 cells and inhibit tumor growth by inhibiting angiogenesis.

In addition to NEP, loss of other membrane-associated peptidases such as CD13/aminopeptidase N and CD26/dipeptidyl peptidase (DPPIV) have been also reported in prostate cancer.[33–35] Recently, Wesley *et al*.[35] reported an inverse relationship between DPPIV and FGF-2 expression in prostate cancer cells. DPPIV-negative DU145 cells showed high FGF-2 expression, while restoration of DPPIV expression resulted in markedly decreased FGF-2 expression,[35] which was similar to our results. Of note, DPPIV-positive LNCaP cells showed low FGF-2 expression, while inhibition of DPPIV expression resulted in increased FGF-2 expression.[35] While these data support

the concept that membrane-associated peptidases such as NEP and DPPIV play an important role in the modulation of FGF-2 production by prostate cancer cells, it is unknown whether DPPIV and NEP coordinately regulate FGF-2 levels.

FGF-2 has been studied extensively in prostate cancer. FGF-2 is present at high concentration in prostate cancer tissues, and believed to function as an autocrine or a paracrine growth factor.[36,37] FGF-2 is one of the most potent angiogenic growth factors. A recent study investigated the relative impact of FGF-2 and VEGF on tumor growth and neovascularization concluded that FGF-2 could promote tumor growth and vascularization even in the presence of a high levels of VEGF.[38] Furthermore, FGF-2 is twice as potent as VEGF at equimolar concentration for stimulating angiogenesis.[39] Based on these studies, it is reasonable to suggest that reduced levels of FGF-2 resulted in significant inhibition of angiogenesis, although VEGF from DU145 cells was sevenfold higher than that of FGF-2 and lentiviral NEP expression had no effect on VEGF levels.

Although adenoviruses are useful as vectors for gene transfer, their critical disadvantage is short-term expression.[40] Long-term expression of anti-angiogenic factors may be necessary for inhibiting tumor growth. Lentivirus vectors are attractive tools for human cancer gene therapy based on their ability to achieve long-term stable expression and maintain therapeutic levels of expression. The present study suggests that lentiviral NEP transduction represents a novel therapeutic strategy for prostate cancer and results in inhibition of FGF-2-mediated angiogenesis.

Acknowledgements

This work was supported by NIH Grants CA80240 and DOD PC040758, and the Robert H McCooey Memorial Cancer Research Fund to DN and NIH grant DA02243 to LBH and Ferdinand C Valentine Fellowship from New York Academy of Medicine to DYTC.

References

1 Shipp MA, Tarr GE, Chen CY, Switzer SN, Hersh LB, Stein H *et al.* CD10/neutral endopeptidase 24.11 hydrolyzes bombesin-like peptides and regulates the growth of small cell carcinomas of the lung. *Proc Natl Acad Sci USA* 1991; **88**: 10662–10666.
2 Turner AJ, Isaac RE, Coates D. The neprilysin (NEP) family of zinc metalloendopeptidases: genomics and function. *Bioessays* 2001; **23**: 261–269.
3 Goodman OG, Febbraio M, Simantov R, Zheng R, Shen R, Silverstein RL *et al.* Neutral endopeptidase inhibits angiogenesis via proteolysis of basic fibroblast growth factor (FGF-2). *J Biol Chem* 2006; **281**: 33597–33605.
4 Papandreou CN, Usmani B, Geng Y, Bogenrieder T, Freeman R, Wilk S *et al.* Neutral endopeptidase 24.11 loss in metastatic human prostate cancer contributes to androgen-independent progression. *Nat Med* 1998; **4**: 50–57.
5 Usmani BA, Shen R, Janeczko M, Papandreou CN, Lee WH, Nelson WG *et al.* Methylation of the neutral endopeptidase gene promoter in human prostate cancers. *Clin Cancer Res* 2000; **6**: 1664–1670.
6 Osman I, Yee H, Taneja SS, Levinson B, Zeleniuch-Jacquotte A, Chang C *et al.* Neutral endopeptidase protein expression and prognosis in localized prostate cancer. *Clin Cancer Res* 2004; **10**: 4096–4100.
7 Sumitomo M, Milowsky MI, Shen R, Navarro D, Dai J, Asano T *et al.* Neutral endopeptidase inhibits neuropeptide-mediated transactivation of the insulin-like growth factor receptor-Akt cell survival pathway. *Cancer Res* 2001; **61**: 3294–3298.
8 Dawson LA, Maitland NJ, Turner AJ, Usmani BA. Stromal–epithelial interactions influence prostate cancer cell invasion by altering the balance of metallopeptidase expression. *Br J Cancer* 2004; **90**: 1577–1582.
9 Osman I, Dai J, Mikhail M, Navarro D, Taneja SS, Lee P *et al.* Loss of neutral endopeptidase and activation of protein kinase B (Akt) is associated with prostate cancer progression. *Cancer* 2006; **107**: 2628–2636.
10 van Bokhoven A, Varella-Garcia M, Korch C, Miller GJ. TSU-Pr1 and JCA-1 cells are derivatives of T24 bladder carcinoma cells and are not of prostatic origin. *Cancer Res* 2001; **61**: 6340–6344.
11 Dai J, Shen R, Sumitomo M, Goldberg JS, Geng Y, Navarro D *et al.* Tumor-suppressive effects of neutral endopeptidase in androgen-independent prostate cancer cells. *Clin Cancer Res* 2001; **7**: 1370–1377.
12 Coleman JE, Huentelman MJ, Kasparov S, Metcalfe BL, Paton JF, Katovich MJ *et al.* Efficient large-scale production and concentration of HIV-1-based lentiviral vectors for use in vivo. *Physiol Genomics* 2003; **12**: 221–228.
13 Marr RA, Rockenstein E, Mukherjee A, Kindy MS, Hersh LB, Gage FH *et al.* Neprilysin gene transfer reduces human amyloid pathology in transgenic mice. *J Neurosci* 2003; **23**: 1992–1996.
14 Pellinen R, Hakkarainen T, Wahlfors T, Tulimaki K, Ketola A, Tenhunen A *et al.* Cancer cells as targets for lentivirus-mediated gene transfer and gene therapy. *Int J Oncol* 2004; **25**: 1753–1762.
15 Bastide C, Maroc N, Bladou F, Hassoun J, Maitland N, Mannoni P *et al.* Expression of a model gene in prostate cancer cells lentivirally transduced *in vitro* and *in vivo*. *Prostate Cancer Prostatic Dis* 2003; **6**: 228–234.
16 Yu D, Chen D, Chiu C, Razmazma B, Chow YH, Pang S. Prostate-specific targeting using PSA promoter-based lentiviral vectors. *Cancer Gene Ther* 2001; **8**: 628–635.
17 Yu D, Jia WW, Gleave ME, Nelson CC, Rennie PS. Prostate-tumor targeting of gene expression by lentiviral vectors containing elements of the probasin promoter. *Prostate* 2004; **59**: 370–382.
18 Zheng JY, Chen D, Chan J, Yu D, Ko E, Pang S. Regression of prostate cancer xenografts by a lentiviral vector specifically expressing diphtheria toxin A. *Cancer Gene Ther* 2003; **10**: 764–770.
19 Morizono K, Xie Y, Ringpis GE, Johnson M, Nassanian H, Lee B *et al.* Lentiviral vector retargeting to P-glycoprotein on metastatic melanoma through intravenous injection. *Nat Med* 2005; **11**: 346–352.
20 Jiang G, Li J, Zeng Z, Xian L. Lentivirus-mediated gene therapy by suppressing survivin in BALB/c nude mice bearing oral squamous cell carcinoma. *Cancer Biol Ther* 2006; **5**: 435–440.
21 Gu W, Putral L, Hengst K, Minto K, Saunders NA, Leggatt G *et al.* Inhibition of cervical cancer cell growth in vitro and in vivo with lentiviral-vector delivered short hairpin RNA targeting human papillomavirus E6 and E7 oncogenes. *Cancer Gene Ther* 2006; **13**: 1023–1032.
22 Sumimoto H, Miyagishi M, Miyoshi H, Yamagata S, Shimizu A, Taira K *et al.* Inhibition of growth and invasive ability of melanoma by inactivation of mutated BRAF with lentivirus-mediated RNA interference. *Oncogene* 2004; **23**: 6031–6039.
23 Goetze S, Bungenstock A, Czupalla C, Eilers F, Stawowy P, Kintscher U *et al.* Leptin induces endothelial cell migration through Akt, which is inhibited by PPARgamma-ligands. *Hypertension* 2002; **40**: 748–754.
24 Shen R, Sumitomo M, Dai J, Harris A, Kaminetzky D, Gao M *et al.* Androgen-induced growth inhibition of androgen receptor expressing androgen-independent prostate cancer cells is mediated by increased levels of neutral endopeptidase. *Endocrinology* 2000; **141**: 1699–1704.

25 Horiguchi A, Sumitomo M, Asakuma J, Asano T, Hayakawa M. 3-hydroxy-3-methylglutaryl-coenzyme a reductase inhibitor, fluvastatin, as a novel agent for prophylaxis of renal cancer metastasis. *Clin Cancer Res* 2004; **10**: 8648–8655.
26 Sumitomo M, Iwase A, Zheng R, Navarro D, Kaminetzky D, Shen R *et al*. Synergy in tumor suppression by direct interaction of neutral endopeptidase with PTEN. *Cancer Cell* 2004; **5**: 67–78.
27 Sumitomo M, Shen R, Walburg M, Dai J, Geng Y, Navarro D *et al*. Neutral endopeptidase inhibits prostate cancer cell migration by blocking focal adhesion kinase signaling. *J Clin Invest* 2000; **106**: 1399–1407.
28 Aoyagi Y, Oda T, Kinoshita T, Nakahashi C, Hasebe T, Ohkohchi N *et al*. Overexpression of TGF-beta by infiltrated granulocytes correlates with the expression of collagen mRNA in pancreatic cancer. *Br J Cancer* 2004; **91**: 1316–1326.
29 Smith JA, Madden T, Vijjeswarapu M, Newman RA. Inhibition of export of fibroblast growth factor-2 (FGF-2) from the prostate cancer cell lines PC3 and DU145 by Anvirzel and its cardiac glycoside component, oleandrin. *Biochem Pharmacol* 2001; **62**: 469–472.
30 Cassinelli G, Lanzi C, Supino R, Pratesi G, Zuco V, Laccabue D *et al*. Cellular bases of the antitumor activity of the novel taxane IDN 5109 (BAY59-8862) on hormone-refractory prostate cancer. *Clin Cancer Res* 2002; **8**: 2647–2654.
31 Turner AJ. Exploring the structure and function of zinc metallopeptidases: old enzymes and new discoveries. *Biochem Soc Trans* 2003; **31**: 723–727.
32 Scholzen TE, Luger TA. Neutral endopeptidase and angiotensin-converting enzyme – key enzymes terminating the action of neuroendocrine mediators. *Exp Dermatol* 2004; **13** (Suppl 4): 22–26.
33 Bogenrieder T, Finstad CL, Freeman RH, Papandreou CN, Scher HI, Albino AP *et al*. Expression and localization of aminopeptidase A, aminopeptidase N, and dipeptidyl peptidase IV in benign and malignant human prostate tissue. *Prostate* 1997; **33**: 225–232.
34 Liu AY, Roudier MP, True LD. Heterogeneity in primary and metastatic prostate cancer as defined by cell surface CD profile. *Am J Pathol* 2004; **165**: 1543–1556.
35 Wesley UV, McGroarty M, Homoyouni A. Dipeptidyl peptidase inhibits malignant phenotype of prostate cancer cells by blocking basic fibroblast growth factor signaling pathway. *Cancer Res* 2005; **65**: 1325–1334.
36 Polnaszek N, Kwabi-Addo B, Peterson LE, Ozen M, Greenberg NM, Ortega S *et al*. Fibroblast growth factor 2 promotes tumor progression in an autochthonous mouse model of prostate cancer. *Cancer Res* 2003; **63**: 5754–5760.
37 Nakamoto T, Chang CS, Li AK, Chodak GW. Basic fibroblast growth factor in human prostate cancer cells. *Cancer Res* 1992; **52**: 571–577.
38 Giavazzi R, Sennino B, Coltrini D, Garofalo A, Dossi R, Ronca R *et al*. Distinct role of fibroblast growth factor-2 and vascular endothelial growth factor on tumor growth and angiogenesis. *Am J Pathol* 2003; **162**: 1913–1926.
39 Nicholson B, Theodorescu D. Angiogenesis and prostate cancer tumor growth. *J Cell Biochem* 2004; **91**: 125–150.
40 MacRae EJ, Giannoudis A, Ryan R, Brown NJ, Hamdy FC, qMaitland N *et al*. Gene therapy for prostate cancer: current strategies and new cell-based approaches. *Prostate* 2006; **66**: 470–494.

Figures

Figure 1. Confluent wildtype (left) and NEP deficient (right) murine vascular endothelial cells micrographs (upper) and stained for DiI-Ac-LDL (lower). B. Anchorage-independent growth of neprilysin-deficient vascular endothelial cells. C. Western blot demonstrating NEP expression as a function of serum concentration in murine vascular endothelial cells. D. Western blot demonstrating basal hyperphosphorylation of ERK in NEP-deficient vascular endothelial cells. Data in A-D are representative of two or more independent experiments.

A.

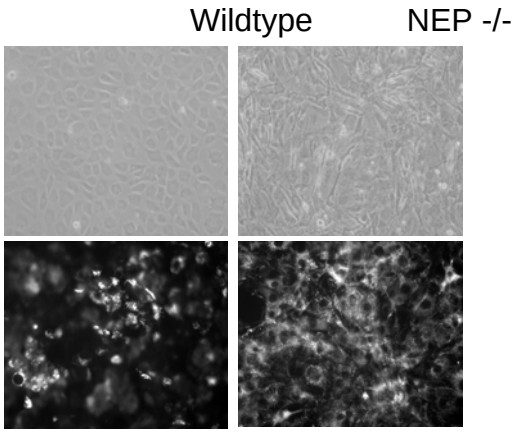

B.

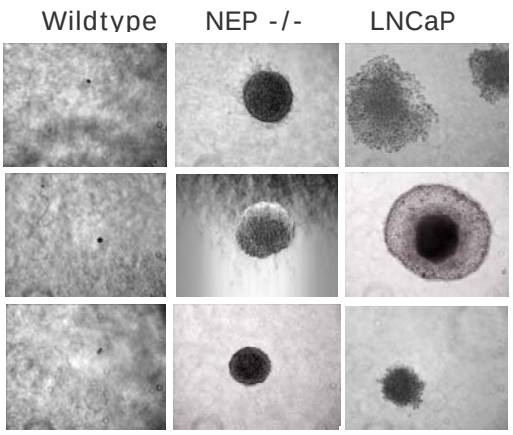

C.

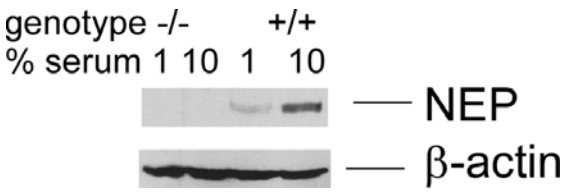

D.

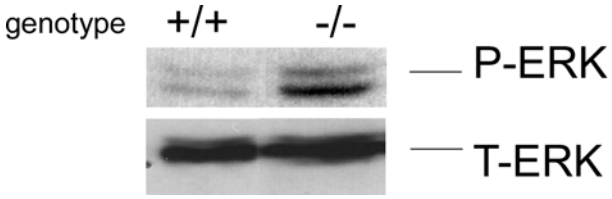

Figures

Figure 2. LNCaP cells or HUVEC cells were plated in 24 well plates and then treated with $CoCl_2$ to a final concentration of 125 μM over the times indicated. Cells were lysed and NEP enzyme activities measured. All time points done in quadruplicate.

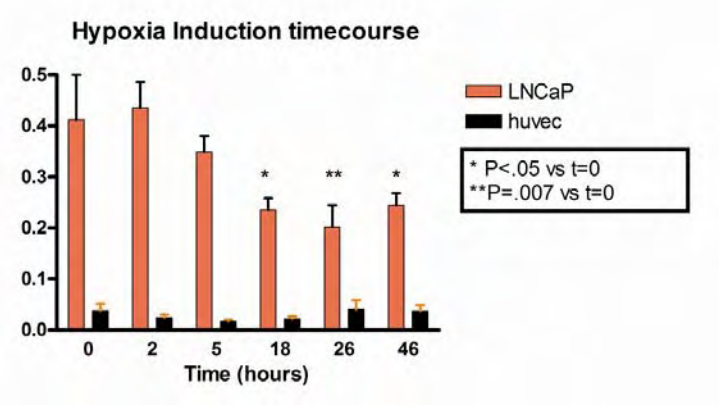

Figure 3. Subconfluent T25 flasks of LNCaP or C4-2 cells were sealed in a hypoxia chamber for 24 hours, lysed in RIPA lysis buffer, and 50 μg lysate analyzed by Western blotting for NEP and β-actin. A 10 ng NEP standard is included (left upper panel).

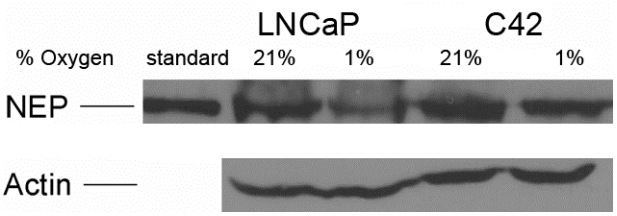

Figure 4. cDNAs (5μg) prepared from normoxic or hypoxia chamber-treated subconfluent LNCaP or C42 cells in T25 flasks were subjected to quadruplicate quantitative real time polymerase chain reaction analysis for NEP, normalized for β-actin expression., and expressed as % of normoxic control. * p= .01, **p=.0001 relative to normoxic control

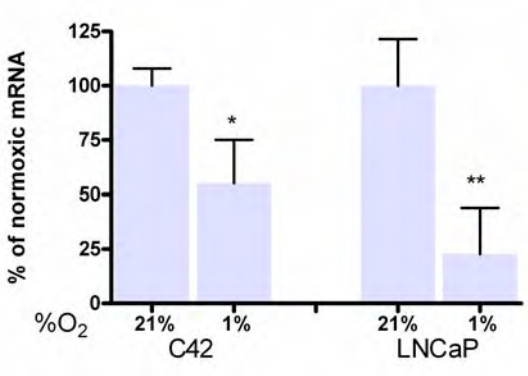

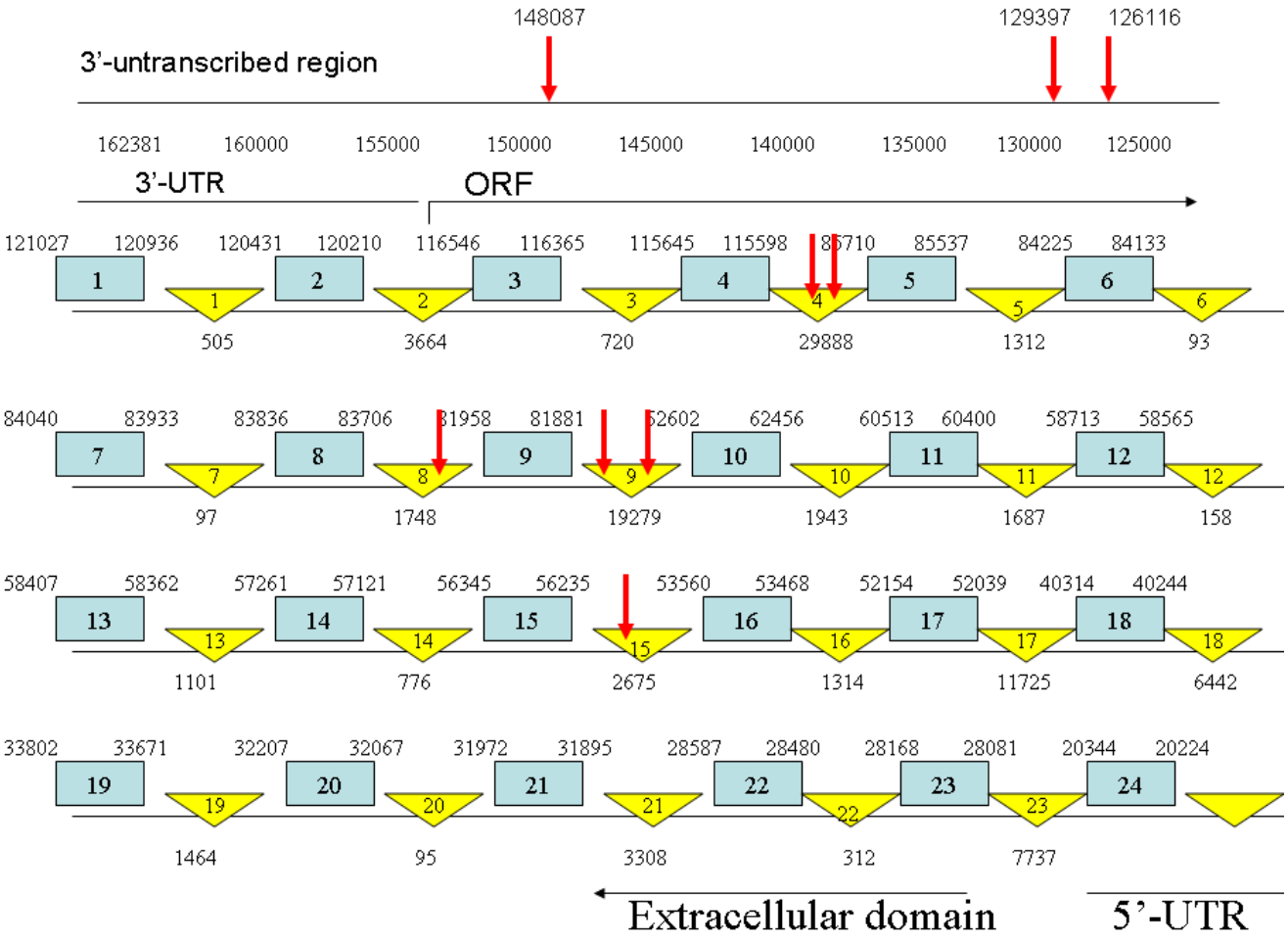
148087
129397
126116
3'-untranscribed region
162381
160000
155000
150000
145000
140000
135000
130000
125000
3'-UTR
ORF
121027
120936
120431
120210
116546
116365
115645
115598
85710
85537
84225
84133
1
2
3
4
5
6
505
3664
720
29888
1312
93
84040
83933
83836
83706
81958
81881
62602
62456
60513
60400
58713
58565
7
8
9
10
11
12
97
1748
19279
1943
1687
158
58407
58362
57261
57121
56345
56235
53560
53468
52154
52039
40314
40244
13
14
15
16
17
18
1101
776
2675
1314
11725
6442
33802
33671
32207
32067
31972
31895
28587
28480
28168
28081
20344
20224
19
20
21
22
23
24
1464
95
3308
312
7737
Extracellular domain
5'-UTR